PHYSIOLOGY AND GENETICS OF DROUGHT TOLERANCE IN COWPEA AND WINTER WHEAT

A Dissertation

by

DAVID ADRIAN VERBREE

Submitted to the Office of Graduate Studies of
Texas A&M University
in partial fulfillment of the requirements for the degree of

DOCTOR OF PHILOSOPHY

May 2012

Major Subject: Plant Breeding

Physiology and Genetics of Drought Tolerance in Cowpea and Winter Wheat

PHYSIOLOGY AND GENETICS OF DROUGHT TOLERANCE IN COWPEA AND WINTER WHEAT

A Dissertation

by

DAVID ADRIAN VERBREE

Submitted to the Office of Graduate Studies of
Texas A&M University
in partial fulfillment of the requirements for the degree of

DOCTOR OF PHILOSOPHY

Approved by:

Co-Chairs of Advisory Committee,	William A. Payne
	Dirk B. Hays
Committee Members,	Jackie Rudd
	Bir B. Singh
Head of Department,	David D. Baltensperger

May 2012

Major Subject: Plant Breeding

ABSTRACT

Physiology and Genetics of Drought Tolerance in Cowpea and Winter Wheat.

(May 2012)

David Adrian Verbree, B.S., Calvin College; M.S., The Pennsylvania State University

Co-Chairs of Advisory Committee: Dr. William A. Payne
Dr. Dirk B. Hays

In the wake of rising temperatures, erratic rainfall, and declining ground water table, breeding for drought tolerance in food crops has become a top priority throughout the world. Phenotyping a large population of breeding lines for drought tolerance is time-consuming and often unreliable due to multiple possible mechanisms involved. In cowpea (*Vigna unguiculata* L. Walp), a box-screening method has been used to partition the confounding effects that shoot and root traits have on drought tolerance by restricting root growth and providing a homogeneous soil moisture environment across genotypes. Nonetheless, multiple mechanisms of shoot drought tolerance have been reported which further complicate phenotyping. In winter wheat (*Triticum aestivum* L.), canopy temperature depression (CTD) has been proposed as a good indicator of drought tolerance. The recent development of low-cost thermal imaging devices could enable high-throughput phenotyping of canopy temperature. While CTD can be an indicator of overall plant water status, it can be confounded by high stomatal resistance, which is another seemingly contradictory mechanism of drought tolerance. The objectives of this study were to explore the physiological basis and genetics of the two mechanisms of

shoot drought tolerance previously reported in cowpea and to develop and evaluate a method of high-throughput phenotyping of drought tolerance in winter wheat using thermal imaging. In cowpea, a legume well known for its tight stomatal control, no differences in gas exchange between drought tolerant and susceptible genotypes were observed. A unifoliate stay-green trait was discovered that segregates as a single recessive gene. However, it did not correlate with trifoliate necrosis or overall drought tolerance. In winter wheat, CTD did not always correlate with yield under rainfed conditions. One drought-tolerant cultivar, in particular, had the hottest canopy temperature, possibly because it was able to conserve moisture by closing its stomata whereas another closely related drought-tolerant cultivar had the coolest canopy temperature. Therefore, it appears that no single method of phenotyping for drought tolerance can be broadly applied across all genotypes of a given species due to possible contrasting mechanisms of drought-tolerance and environmental differences.

DEDICATION

To the impoverished who provide an endless source of motivation to use this degree ultimately to help improve food security and alleviate their suffering.

ACKNOWLEDGEMENTS

I would like to thank my family who have supported me through much uncertainty and continue to do so and my committee chair, Dr. William "Bill" Payne, whose passion for international development work and ability to stay positive in the midst of difficult circumstances has been a great encouragement to me. I would also like to thank my committee members, Dr. Dirk Hays, Dr. Jackie Rudd, and Dr. B.B. Singh and my collaborators, Dr. Qingwu Xue and staff (AgriLife Research in Amarillo, TX), Dr. Maria Balota (Virginia Tech), Dr. Steve Evett and staff (USDA-ARS in Bushland, TX), and Jeff Ehlers (University of California – Riverside) and staff. Lastly, I would like to thank everyone who supported our cowpea field operations at the AgriLife Research Agronomy Farm in College Station, TX including our Farm Manager, Al Nelson, and staff, Dr. Bill Rooney and the Texas A&M Sorghum Program and the Texas A&M Cowpea Group.

This research was conducted on behalf of the Soil and Crop Department, the Normal Borlaug Institute of International Agriculture, and AgriLife Research of Texas A&M University with our partners at the University of California – Riverside and USDA-ARS at Bushland, Texas. It was made possible through funding from the Consultative Group on International Agricultural Research (CGIAR) Generation Challenge Program, The McKnight Foundation, the Ogallala Aquifer Research Consortium, the Wheat Producers Board, an assistantship from the Texas A&M Department of Soil and Crop Sciences, and a Texas A&M Diversity Fellowship.

TABLE OF CONTENTS

Page

Page

Page

LIST OF FIGURES

Page

Page

LIST OF TABLES

Page

Page

Page

1. INTRODUCTION

The 21st century is experiencing the combined effect of population growth and climate change leading to an unsustainable and insecure use of food and water resources. Climate change experts predict an increase in temperatures and frequency of severe events such as droughts and floods (Kundzewicz et al. 2008). Higher temperatures may increase precipitation but also increase evaporation from cropland and surface water. An increase in the frequency of droughts and floods that destroy crops can have a devastating effect on food prices and availability. Breeding for drought tolerance reduces the risk of crop failure by improving its ability to extract water from the soil (deeper or more fibrous roots), decreasing the amount of water a crop demands (e.g. improving its water use efficiency), or by improving a crop's ability to survive longer periods without water, thereby ultimately increasing yields in rainfed environments. Efforts to breed for drought tolerance are hampered by the amount of time required to phenotype a large number of individuals and poor or inconsistent correlation between a phenotype and yield under drought conditions due, in part, to multiple mechanisms involved.

Cowpea (*Vigna unguiculata* L. Walp) is one of the world's most drought-tolerant grain legumes. However, most U.S. cultivars are less tolerant to water stress than many African cultivars. Efforts are currently underway to breed enhanced drought-tolerance from African cultivars into U.S. cultivars. Determining the genetic control and elucidating the mechanisms of drought tolerance in cowpea may accelerate these efforts

---

This dissertation follows the style of Crop Science.

and assist breeders, molecular scientists, and geneticists to improve drought tolerance in other important legumes.

Winter wheat (*Triticum aestivum* L.) is one of the world's most important grains. It is commonly produced in both irrigated and rainfed environments. However, declining fresh water availability in many regions and increasing costs of irrigation are causing producers to reduce their dependence on irrigation either by shifting to deficit irrigation or by eliminating irrigation altogether. Therefore, improving drought tolerance of wheat under rainfed conditions has become a top priority for breeders. Phenotyping a large number of breeding lines for drought tolerance can be difficult, time-consuming, and unreliable. Canopy temperature depression (CTD) has been proposed as a good indicator of drought tolerance. The recent development of low-cost thermal imaging devices could enable high-throughput phenotyping of canopy temperature. However, a method of using a thermal imaging device to assess canopy temperatures of winter wheat cultivars under field conditions and an efficient method to analyze thermal images have not been developed. Further, there are questions regarding the interpretation of canopy temperature with respect to drought tolerance and yield for breeding purposes.

2. GENETICS AND HERITABILITY OF SHOOT DROUGHT TOLERANCE IN COWPEA

2.1 Introduction

Breeding for drought tolerance in legumes has become a top priority especially in developing nations plagued by low and erratic rainfall and with high incidence of malnutrition (Global Development Program, 2011). While common staple grain crops such as maize and wheat have received much attention from breeders, these crops do not meet all essential nutritional needs for human consumption and are not all suited for extreme environments. Cowpea [*Vigna unguiculata* (L.) Walp], one of the most drought-tolerant legumes (Graham and Vance, 2003), is capable of producing a crop with less than 500 mm of rainfall, is highly nutritious, fixes nitrogen, and mature quickly. It is commonly produced and consumed in developing countries including most of Africa. It is also an important crop in the United States, especially in Texas and California. Unfortunately, most U.S. cultivars are not as drought-tolerant as African cultivars possibly due to a genetic bottleneck that likely occurred during domestication or migration (Fang et al. 2007). In view of the increased incidence of drought and reduced availability of fresh water resources, attempts are being made to incorporate enhanced drought tolerance from African cultivars into U.S. cultivars.

Previous research suggests that there are two unique responses to water stress among drought-tolerant cowpea cultivars (Mai-Kodomi et al., 1999a). For “type 1” cultivars, growth is arrested, moisture is conserved, and the unifoliates and trifoliates

desiccate at approximately the same time, whereas for "type 2" cultivars, moisture is conserved for a longer time and growth continues slowly for the youngest trifoliate but the unifoliates desiccate early. The conservation of moisture in both types of cultivars is likely due to high stomatal resistance. However, the reduction of leaf area in type 2 cultivars could be an additional mechanism of drought tolerance by which transpirational losses are reduced. Both types of drought tolerance were found to be dominant over drought susceptibility and both were controlled by a single dominant gene. However, a cross between type 1 and type 2 showed the dominance of type 1 with monogenic inheritance indicating that the two types are controlled by alleles at the same locus (Mai-Kodomi et al., 1999b). If either trait is controlled by a single gene, breeding drought tolerance of either form into susceptible cultivars should be an easy task. Furthermore, a mapping population could be used to identify markers for those genes to assist breeders in developing improved cultivars or to map the genes that could then be transformed into other drought susceptible legumes.

Possible contrasting mechanisms of drought tolerance may require multiple phenotypes to be assessed for each individual. The quickest method to screen numerous genotypes is by rating individuals for visual traits such as wilting, chlorosis, and necrosis. The finding of Mai-Kodomi et al. (1999a) suggests that the both the unifoliates and trifoliates of cowpea must be rated separately to determine the type of drought tolerance. In several species including soybean, stem diameter has been found to decrease in response to water stress, even diurnally (Ohashi et al., 2006; Simoneau et al.,

1993; Hinckley and Bruckerhoff, 1975). Therefore, stem diameter, which is quick and easy to phenotype, may be a good indicator of drought tolerance in cowpea as well.

The goal of this study was to screen a large number of cowpea cultivars, determine the best phenotypic predictors of drought tolerance, identify susceptible and tolerant type 1 and type 2 cultivars, and develop mapping populations to confirm the genetics and heritability of both forms of drought tolerance.

2.2 Materials and methods

2.2.1 Phenotyping cultivars for shoot drought tolerance

Cowpea seedlings were screened in shallow boxes to reduce differences in root morphology using a method similar to that described by Singh et al. (1999). One cm diameter drain holes were drilled in a 7.5-cm grid pattern in the bottom of ten, 39-L Sterilite® polypropylene boxes (model 1960, Sterilite Corporation, Townsend, MA; 88.6 cm L x 42.2 cm W x 15.6 cm H). Each box was filled with Metro-mix® 700 planting media (Sun Gro Horticulture Canada CM Ltd., Vancouver, British Columbia, Canada) which is a coarse mix of composted pine bark, sphagnum peat moss, vermiculite, and perlite. The media is highly resistant to settling and provided a relatively uniform water holding capacity across the containers. The boxes were moved into a growth room set to 12-hour days, 33°C daytime temperature, and 24°C nighttime temperature for the duration of the experiment. Each box was watered thoroughly and allowed to sit for two days until the soil was approximately at field capacity. Ten rows (five rows per replication) of six hills were marked out in each box, 7.5 cm between rows and 5.0 cm

between holes. Four cultivars and a common check (TVu-7778 from IITA) were planted 2.5 cm deep, one cultivar per row and two seeds per hill. The order of the cultivars in the second replication was shifted over three rows in order to reduce bias due to possible edge-of-box effects. As soon as the first unifoliates were fully expanded, the boxes were thinned to one plant per hole and watered a final time.

The number of lodged plants and the number of plants with wilted unifoliates, wilted trifoliates, necrotic unifoliates, necrotic trifoliates, and dead growing points were recorded every three days for each cultivar until most of the plants were dead. The number of days until: a) 33% of the plants were lodged, b) 50% were dead (LD50), c) 50% had wilted unifoliates, d) 50% had wilted trifoliates, e) 50% had necrotic unifoliates, and f) 50% had necrotic trifoliates (TN50) were calculated for each cultivar. The stem diameter was also measured for each plant, 1.0 cm above the soil surface, at the first sign of wilting using a digital caliper.

Statistics were performed on these data using SAS® 9.2 for Windows (SAS Institute Inc. Charlotte, NC). The data was analyzed as an augmented design using a general linear model as per Scott and Milliken (1993). Fisher's least significant differences (LSDs) were calculated manually using the standard formula.

2.2.2 Developing and phenotyping mapping populations

The most drought susceptible and type 1 and type 2 drought tolerant cultivars were selected based on the box screening experiment for further evaluation. The drought susceptible cultivars were hybridized to tolerant cultivars to produce F_1 seed. The F_1 seed was inbred to produce F_2 seed. Eighty F_2 seeds of each family were planted, 40

seeds per box, to screen for shoot drought tolerance in a greenhouse using a method similar to that described in Section 2.2.1. Four seeds of each parent were also planted in random locations in each box as checks. The boxes were watered until the first unifoliate was fully expanded. Water was withheld and the proportion of progeny with unifoliates that turned yellow during senescence were determined as well as the proportion of plants with green fully-expanded trifoliates once segregation was evident and the counts were stable for approximately one week. One F_2 family (TX2028-1-3-1/CB46) that showed excellent 1:3 segregation for unifoliate greenness was selected for an F_3-generation study. Each F_2 plant was individually identified, re-watered, and transplanted into 7.6-L pots. F_3 seed was harvested from each plant. Twelve F_3 seeds from each of 12 susceptible and 6 tolerant F_2 plants were planted and screened for drought tolerance in a similar fashion as the F_2 seed. Progeny rows from 2 susceptible and 1 resistant F_2 plants and a row of the resistant and susceptible parents as checks were planted in each of 6 boxes.

2.3 Results and discussion

2.3.1 Phenotyping cultivars

The augmented design resulted in a significant partitioning out of environmental variance into both the box variance and the check variance for all indicators of drought tolerance evaluated as response variables except number of days until half died (LD50) and the number of days until one-third lodged (ANOVA table for trifoliate necrosis shown in Table 2.1). This environmental variance was due to a temperature gradient

across the length of the growth room that resulted in an observed differential drying of the soil boxes. Therefore, all results are reported as adjusted means.

Table 2.1. Analysis of variance for seedling box screening of 40 cowpea cultivars for trifoliate necrosis under growthroom terminal-drought conditions using an augmented design.

Source	DF	Type 3 SS	MS	F Value	Pr >F
box	9	88.20	9.80	3.45	0.0034
check	1	354.65	354.65	124.78	<0.0001
cultivar(check)	31	411.99	13.29	4.68	<0.0001
Error	38	108.00	2.84		
Total	79	899.55			

The LD50 was based on the number of days since last watering until half of the plants either were lodged or had necrotic growing points. It was not significantly different by genotype and was likely confounded by a stay-green phenomena experienced in several cultivars whereby the growing point appeared green even after complete necrosis of all of the leaves. It is therefore unlikely that plants with this trait would survive upon re-watering. Resistance to trifoliate necrosis and differences in stem diameter were both better able to differentiate between cultivars than LD50.

Trifoliate necrosis (TN50) was significantly different by genotype (Table 2.2) and significantly correlated with death (LD50; r = 0.773). The TN50 measurement takes into account the same factors as LD50 but also considers the number of plants with necrotic trifoliates. It reflects the proportion of plants that have lost their photosynthetic ability or are otherwise unlikely to survive and, therefore, may be a more accurate and consistent indicator of seedling death than LD50.

Table 2.2. Number of days until unifoliate and trifoliate necrosis and the difference in days between them for cowpea cultivars grown in shallow boxes in a growth room under terminal water stress.

days to 50% unifoliate necrosis		days to 50% trifoliate necrosis		days to 50% tri – uni necrosis	
cultivar	adjusted means	cultivar	adjusted means	cultivar	adjusted means
	— days —		— days —		— days —
TX2028-1-3-1	40	TX2028-1-3-1	*	TX2028-1-3-1	*
CB27	38	CB27	*	CB27	*
Bambey 21	38	Sh-50	*	Sh-50	*
CRSP Niebe	37	524 B	*	524 B	*
Sh-50	36	P-24	*	P-24	*
IT99K-407-8	36	CC-36	*	CC-36	*
IT98K-205-8	36	CC-27	*	CC-27	*
UCR 288	36	IT99K-241-2	*	IT99K-241-2	*
N'diambour	36	Kvx 421-25	51	Kvx 421-25	18
524 B	35	Kvx 525	51	Kvx 525	18
Apagbaala	35	UCR 288	48	Dan Ila	17
IT97K-556-4	35	Kvx 403	48	Kvx 61-1	16
UCR 1432	35	Dan Ila	48	Kvx 403	15
Iron Clay	35	CRSP Niebe	47	Kvx 396	15
P-24	34	IT97K-556-4	47	Mouride	14
CB46	34	CB46	47	CB46	13
IT98D-1399	34	IT98D-1399	47	IT98D-1399	13
24-1258-1	34	Kvx 61-1	47	Mounge	13
CC-36	34	IT98K-205-8	45	UCR 799	13
Kvx 421-25	33	Iron Clay	45	IT98K-128-2	13
Kvx 403	33	24-1258-1	45	UCR 288	12
Melakh	33	Mounge	45	IT97K-556-4	12
IT98K-498-1	33	UCR 799	45	Ife Brown	12
Kvx 525	33	IT98K-128-2	45	58-57	12
Suvita 2	33	Kvx 396	45	24-1258-1	11
CC-27	32	Suvita 2	44	Suvita 2	11
Mounge	32	Mouride	44	Yacine	11
UCR 5272	32	N'diambour	42	TVu7778	11
UCR 799	32	Apagbaala	42	CRSP Niebe	10
IAR7/8-5-4-1	32	UCR 1432	42	Iron Clay	10
IT98K-128-2	32	Melakh	42	UCR 5272	10
Dan Ila	31	UCR 5272	42	58-53	10
58-53	31	Yacine	42	IT98K-205-8	9
Yacine	31	Ife Brown	42	Melakh	9
Kvx 61-1	31	IT99K-407-8	41	IAR7/8-5-4-1	9
IT99K-241-2	31	IAR7/8-5-4-1	41	Apagbaala	7
Kvx 396	30	58-53	41	UCR 1432	7
Ife Brown	30	58-57	41	N'diambour	6
Mouride	30	TVu7778	39	IT99K-407-8	5
58-57	29	Bambey 21	38	IT98K-498-1	3
TVu7778	28	IT98K-498-1	36	Bambey 21	0
Mean	32.5	Mean	42.6	Mean	10.8
CV (%)	4.7	CV (%)	4.2	CV (%)	18.1
LSD (5%)	3.10	LSD (5%)	3.70	LSD (5%)	4.00

* Completely resistance to necrosis for the duration of the experiment.

Stem diameter (Table 2.3), measured at the first sign of wilting, was significantly correlated with days until unifoliate and trifoliate necrosis (r = 0.600 and 0.511, respectively) although it was not as well correlated with days until unifoliate or trifoliate wilting (r = 0.471 and 0.422, respectively). Therefore, it is possible that in cowpea, stem diameter more closely reflects changes in carbohydrates stored in the stem than the plant's water status, as suggested by Ohashi et al. (2006) for soybean. Indeed, an internal pithiness or hollowing of the stem and petiole was observed during advanced stages of water stress suggesting that remobilization of carbohydrates may have taken place. During grain-filling, Gwathmey et al. (1992) found that sucrose increased in the stems of cowpea cultivars with a delayed leaf senescence trait whereas the non-structural carbohydrates were depleted in the stems of cultivars without that trait. Similarly, Crafts-Bradner et al. (1984) found that the stem and leaves of soybeans served as an alternate carbohydrate sink when the pods were removed. It is possible that the stem of cowpea serves as a carbohydrate reserve not only during grain filling when the demand is high but also during water stress when photosynthesis is reduced. During water stress, glucose and ATP produced from stored carbohydrates are needed to synthesize important antioxidants such as ascorbate and glutathione to protect the plant against free radicals thereby delaying the onset of necrosis or program cell death (Noctor and Foyer, 1998).

Table 2.3. Stem diameter of cowpea cultivars grown in shallow boxes in a growth room under terminal water stress.

cultivar	stem dia.
	—— mm ——
Sh-50	3.15
CB27	3.13
524 B	3.01
P-24	2.99
24-1258-1	2.83
IT99K-241-2	2.82
IT99K-407-8	2.81
Melakh	2.80
CRSP Niebe	2.72
CC-27	2.66
Yacine	2.59
Mouride	2.58
IT98K-128-2	2.57
Suvita 2	2.57
IT97K-556-4	2.54
Ife Brown	2.54
58-53	2.54
Dan Ila	2.51
N'diambour	2.51
Mounge	2.48
Kvx 403	2.47
CB46	2.47
TX2028-1-3-1	2.43
CC-36	2.43
58-57	2.40
UCR 799	2.39
Bambey 21	2.37
Kvx 421-25	2.34
Apagbaala	2.34
UCR 1432	2.32
IT98K-205-8	2.30
Kvx 525	2.27
IT98K-498-1	2.24
UCR 5272	2.23
Kvx 61-1	2.21
UCR 288	2.17
IT98D-1399	2.16
IAR7/8-5-4-1	2.13
Iron Clay	1.99
Kvx 396	1.84
TVu7778	1.82
Mean	2.36
CV (%)	6.43
LSD (5%)	0.305

Stem diameter was also significantly correlated with days until lodging (r = 0.572) and lodging was found to be a significant cause of death in young seedlings (r = 0.634) most notably for the drought susceptible control, TVu-7778. However, several other factors influence lodging susceptibility such as cellulosic content (York et al., 1990; York and Hawkins, 2000; Kokubo et al., 1989 and 1991; Taylor et al. 1999) or dry matter per unit length (Hashemi et al., 2003) which both account for stem pithiness.

IT99K-241-2 and TX2028-1-3-1 (Figure 2.1) were both highly resistant to trifoliate necrosis and are therefore drought tolerant (Table 2.2). IT99K-241-2 was one of the most susceptible to unifoliate necrosis (Type 2 tolerance) whereas TX2028-1-3-1 was the most resistant to unifoliate necrosis (Type 1 tolerance), illustrating the two types of drought tolerance suggested by Mai-Kodomi et al. (1999a). Even though TX2028-1-3-1 was one of the most resistant to unifoliate necrosis, it was one of the most susceptible to unifoliate wilting (Table 2.4). Therefore, the unifoliate stay-green trait may be independent of the "type 1" drought tolerance reported by Mai-Kodomi et al. (1999a) and by itself may not confer drought tolerance.

Bambey 21 and TVu-7778 were among the most susceptible to trifoliate necrosis (Table 2.2). However, they contrasted sharply in their resistance to unifoliate necrosis similar to the drought tolerant cultivars, IT99K-241-2 and TX2028-1-3-1. Bambey 21 was among the most tolerant to unifoliate necrosis whereas TVu-7778 was the most susceptible to unifoliate necrosis. Therefore, it appears that the unifoliate stay-green trait can be present even in a drought-susceptible cultivar, such as Bambey 21, and by itself may not confer drought tolerance.

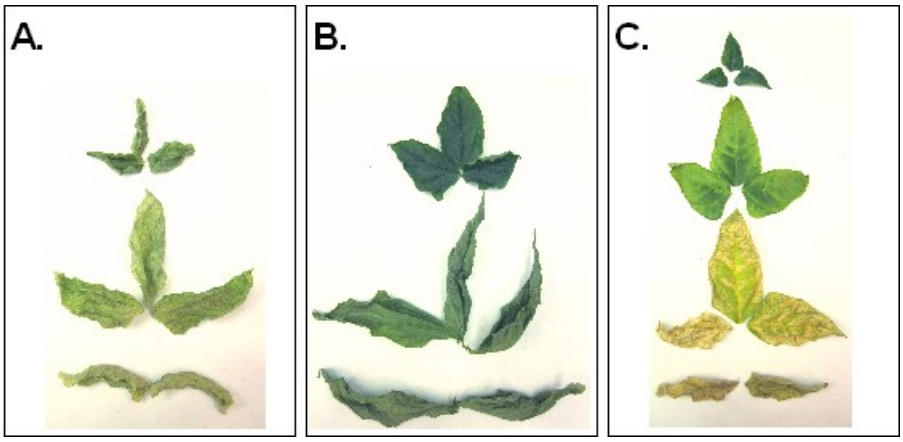

Figure 2.1. Contrasting responses of cowpea cultivars to water stress. A. The unifoliates and trifoliates of the drought susceptible cultivar, TVu-7778, are both susceptible to necrosis. B. The unifoliates and trifoliates of the drought tolerant cultivar, TX2028-1-3-1, are both resistant to necrosis. C. The unifoliates of the "type 2" drought-tolerant cultivar, IT99K-241-2, are susceptible to necrosis whereas the youngest trifoliates are resistant.

Table 2.4. Number of days until unifoliate wilting, the number of days until trifoliate wilting, and the difference in the number of days between unifoliate and trifoliate wilting of cowpea cultivars grown in shallow boxes under terminal water

days to 50% unifoliate wilt		days to 50% trifoliate wilt		days to 50% tri – uni wilt	
cultivar	adjusted means	cultivar	adjusted means	cultivar	adjusted means
	— days —		— days —		— days —
IT99K-241-2	36	IT99K-241-2	*	IT99K-241-2	*
CB46	35	Suvita 2	*	Suvita 2	*
CB27	34	TX2028-1-3-1	*	TX2028-1-3-1	*
P-24	34	Kvx 421-25	49	Kvx 421-25	19
524 B	33	CB27	47	P-24	17
Apagbaala	33	P-24	47	Dan Ila	15
CRSP Niebe	33	Dan Ila	47	CB27	14
Dan Ila	33	524 B	44	58-53	13
IAR7/8-5-4-1	33	CB46	43	524 B	12
IT98D-1399	33	Sh-50	43	Sh-50	11
Kvx 61-1	33	IT98D-1399	41	Kvx 403	11
Melakh	33	58-53	41	CB46	8
24-1258-1	32	CRSP Niebe	38	IT98D-1399	8
CC-36	32	Melakh	38	Bambey 21	7
Sh-50	32	Bambey 21	38	CRSP Niebe	6
Bambey 21	31	Kvx 403	38	Melakh	6
Iron Clay	31	IAR7/8-5-4-1	37	CC-27	6
IT98K-128-2	31	24-1258-1	37	IT99K-407-8	6
N'diambour	31	CC-27	36	Yacine	6
CC-27	30	Apagbaala	35	24-1258-1	5
IT97K-556-4	30	CC-36	35	IT98K-205-8	5
IT99K-407-8	30	IT98K-128-2	35	Kvx 396	5
Kvx 421-25	30	IT99K-407-8	35	IT98K-498-1	5
Mouride	30	Yacine	35	Mounge	5
Suvita 2	30	IT98K-205-8	34	TVu7778	5
58-57	29	Kvx 396	34	UCR 5272	5
Ife Brown	29	Iron Clay	32	UCR 799	5
IT98K-205-8	29	IT97K-556-4	32	IAR7/8-5-4-1	4
Kvx 396	29	58-57	32	IT98K-128-2	4
TX2028-1-3-1	29	IT98K-498-1	32	Apagbaala	3
Yacine	29	Mounge	32	CC-36	3
58-53	28	TVu7778	32	IT97K-556-4	3
IT98K-498-1	28	UCR 5272	32	58-57	3
Kvx 403	28	UCR 799	32	Kvx 525	3
Kvx 525	28	Kvx 61-1	31	Ife Brown	2
Mounge	28	N'diambour	31	UCR 1432	2
TVu7778	28	Mouride	31	UCR 288	2
UCR 1432	28	Ife Brown	31	Iron Clay	1
UCR 288	28	Kvx 525	31	Mouride	1
UCR 5272	28	UCR 1432	29	N'diambour	0
UCR 799	28	UCR 288	29	Kvx 61-1	-2
Mean	29.9	Mean	34.9	Mean	5.0
CV (%)	4.6	CV (%)	7.3	CV (%)	47.5
LSD (5%)	2.80	LSD (5%)	5.20	LSD (5%)	5.30

* Completely resistance to wilt for the duration of the experiment.

2.3.2 Developing and phenotyping mapping populations

Crosses were made between both types of drought tolerant cultivars, TX2028-1-3-1 and IT99K-241-2, and the most drought susceptible cultivar, TVu-7778, as well as a moderately drought susceptible cultivar, CB46. CB46 is one of the most common cultivars produced commercially in the United States. It was moderately susceptible to both unifoliate necrosis and trifoliate necrosis (Table 2.2) but unlike TVu-7778, it was resistant to both unifoliate wilting and trifoliate wilting (Table 2.4). Crosses were also made between the two drought tolerant cultivars, TX2028-1-3-1 and IT99K-241-2, to determine if the types of drought tolerance could be combined.

The crosses between the drought tolerant cultivar, TX2028-1-3-1, and both susceptible cultivars, TVu-7778 and CB 46, produced F_2 progeny that showed excellent 1:3 segregation for the unifoliate stay-green trait (Table 2.5) despite the fact that CB46 was much more resistant to wilting than TVu-7778. Approximately, 29%, 28%, and 30% of the F_2 progeny were resistant to unifoliate necrosis for the crosses TX2028-1-3-1/CB46, CB46/TX2028-1-3-1 (reciprocal cross), and TX2028-1-3-1/TVu-7778, respectively. This suggests that the unifoliate stay-green trait is controlled by a single recessive gene. It further suggests that this trait may be unrelated to the single dominant gene that confers type 1 drought tolerance as reported by Mai-Kodomi et al. (1999a). The F_2 progeny of TX2028-1-3-1 crossed with IT99K-241-2, the type 2 drought tolerant cultivar, did not segregate 1:3 for the unifoliate stay-green trait, as did the other populations. Rather, the proportion of progeny resistant to unifoliate senescence was far

greater likely, because the unifoliate stay-green trait was confounded by the much greater degree of overall drought tolerance imparted by IT99K-241-2.

The F_3 segregation ratios for unifoliate necrosis of 6 resistant and 12 susceptible F_2 plants confirmed that the unifoliate stay-green trait is controlled by a single recessive gene (Table 2.6). All 12 progeny from each of the 6 resistant cultivars had the unifoliate stay-green trait whereas all 12 progeny from 4 of the 12 susceptible F_2 plants were susceptible. The progeny from the remaining 8 susceptible F_2 parents segregated approximately 1:3 (23:73 combined) for resistance to the unifoliate stay-green trait as was found in the F_2 screening.

Segregation of resistance to trifoliate necrosis was much less discernible than that of resistance to unifoliate necrosis (Table 2.5). For example, the parental checks, TX2028-1-3-1 and TVu-7778, in the box screening of their F_2 progeny recovered 100% and 0% of the unifoliate stay-green trait, respectively, whereas 38% and 25% of each parent were classified as resistant to trifoliate necrosis, respectively. The same ratios of trifoliate necrosis were found for the type 2 drought tolerant cultivar, IT99K-241-2, and the same highly susceptible cultivar, TVu-7778. Apparently, the greenhouse conditions were not suitable to replicate the strong contrasts in trifoliate necrosis between the drought tolerant and susceptible parents as were evident under growth room conditions. The daytime temperature in the greenhouse was warmer, the humidity lower, and the day-length longer than growth room conditions, thereby accelerating water stress making differentiation between susceptible and tolerant cultivars more difficult.

Table 2.5. Segregation ratios of F_2 recombinant inbred lines for unifoliate, trifoliate, and stem necrosis.

	F_2 Progeny			
Cross	No. susceptible	No. resistant	X^2	P-value
	unifoliate necrosis*			
TX2028-1-3-1/CB46	63	26	0.843	0.359
CB46/TX20281-3-1	55	24	1.219	0.269
TX2028-1-3-1/TVu-7778	56	24	1.067	0.302
IT99K-241-2/TX2028-1-3-1	16	64	131.409	0.000
	trifoliate necrosis†			
CB46/TX20281-3-1	32	47	10.131	0.001
TX2028-1-3-1/TVu-7778	44	36	38.400	0.000
IT99K-241-2/TX2028-1-3-1	21	59	0.067	0.796
IT99K-241-2/TVu-7778	29	51	5.400	0.020
	stem necrosis*			
CB46/TX2028-1-3-1	57	22	0.342	0.559
TX2028-1-3-1/TVu-7778	12	68	153.600	0.000

* X^2 and p-values for unifoliate necrosis and stem necrosis are for a test of the null hypothesis that F_2 progeny segregate in a 3 susceptible to 1 resistant ratio.
† X^2 and p-values for trifoliate necrosis are for a test of the null hypothesis that F_2 progeny segregate in a 3 resistant to 1 susceptible ratio.

Table 2.6. Segregation ratios of F3 progeny from TX2028-1-3-1/CB46 that were susceptible and resistant to unifoliate necrosis.

F_2 parent		F_3 progeny			
ID	Phenotype	No. susceptible	No. resistant	X^{2}*	P-value*
3-2	susceptible	8	4	0.444	0.505
7-5	susceptible	9	3	0.000	1.000
4-6	resistant	0	12	true-breeding	-
2-4	susceptible	12	0	true-breeding	-
6-4	susceptible	10	2	0.444	0.505
8-2	resistant	0	12	true-breeding	-
5-3	resistant	0	12	true-breeding	-
1-3	susceptible	11	0	true-breeding	-
5-1	susceptible	10	2	0.444	0.505
1-2	susceptible	10	0	true-breeding	-
3-3	resistant	0	12	true-breeding	-
4-5	susceptible	12	0	true-breeding	-
8-6	resistant	0	12	true-breeding	-
4-3	susceptible	8	4	0.444	0.505
7-1	susceptible	9	3	0.000	1.000
8-1	resistant	0	12	true-breeding	-
3-5	susceptible	11	1	1.778	0.182
5-4	susceptible	8	4	0.444	0.505

* X^{2} and p-values are for a test of the null hypothesis that F_3 progeny segregate in a 3 susceptible:1 resistant ratio.

Despite somewhat poor recovery of the parental phenotypes for trifoliate necrosis under greenhouse conditions, the F_2 progeny for two of the crosses (IT99K-241-2/TX2028-1-3-1 and IT99K-241-2/TVu-7778) segregated more like a single dominant gene in accordance with Mai-Kodomi et al. (1999a) than a single recessive gene. Approximately 74% and 64% of the F_2 progeny of the crosses between the most tolerant type 2 and type 1 cultivars (IT99K-241-2 and TX2028-1-3-1, respectively) and the most susceptible cultivar (TVu-7778) were resistant to trifoliate necrosis (Table 2.5). There were no significant correlations between unifoliate and trifoliate necrosis for the F_2

progeny of any cross, which confirms the results of the parent line box screening experiment.

2.4 Conclusions

Trifoliate necrosis was found to be the most reliable indicator of overall shoot drought tolerance in cowpea. Lodging was a major cause of death in cowpea even under still growth room conditions. Stem diameter was highly correlated with resistance to lodging, and with unifoliate and trifoliate necrosis but not as well correlated with resistance to wilting, suggesting that carbohydrates stored in the stem may help to mitigate water stress. A unifoliate stay-green trait was discovered which segregates as a single recessive gene. However, it did not co-segregate with resistance to trifoliate necrosis. Therefore, this trait likely does not confer drought tolerance and may be unrelated to the single dominant gene for drought tolerance reported by Mai-Kodomi et al. (1999a). The contrasting parental phenotypes for resistance to trifoliate necrosis evident in the growth room could not be fully recovered under the greenhouse conditions. Therefore, no repeatable segregation patterns were observed for resistance to trifoliate necrosis or “type 2” drought tolerance.

3. PHYSIOLOGY OF DROUGHT TOLERANCE IN COWPEA

3.1 Introduction

Drought tolerance is the ability of a plant to survive periods with insufficient uptake of water. Several mechanisms of drought tolerance in cowpea have been suggested including paraheliotropism to avoid photoinhibition (Schakel and Hall, 1979), increased stomatal resistance to reduce water lost by transpiration (Auge et al. 1992; Anyia and Herzog 2004; Bates and Hall, 1981 and 1982; Cruz de Carvalho et al., 1998; Hamidou et al. 2007; Hall and Schulze 1980; Souza et al., 2004), reduction of leaf area (Hall and Schulze 1980) which also reduces transpiration losses, increased antioxidant activity to reduce reactive oxidative species (Contour-Ansel et al. 2006; Manivannan et al. 2007), and differential regulation of alternative oxidase activity (Costa et al. 2007). However, decades of research have yet to produce an integrated view of drought tolerance in cowpea that can enable breeders to select for suitable traits more effectively.

Mai-Kodomi et al. (1999a) suggested that multiple mechanisms of drought tolerance exist within cowpea germplasm but that it may be difficult to combine all the traits into a single cultivar. Specifically, they identified two unique responses to water stress in cowpea: In type 1 response, growth was arrested, moisture was conserved, and the unifoliates and trifoliates desiccated at the same time. In type 2 response, the unifoliates desiccated early and leaf moisture was conserved to allow growth to continue slowly for the youngest trifoliate. No published research has since elaborated on the physiological basis of each of these mechanisms.

In the study described in Section 2, 40 cowpea cultivars from several countries were screened, ranked, and classified as to their mechanism and level of drought tolerance. This was done in shallow boxes to reduce root effects and provide a common soil moisture environment. Strong contrasts in the level and type of drought tolerance were found between cultivars under these conditions suggesting that the shoot may be just as important as the roots in conferring drought tolerance in cowpea. Resistance to trifoliate necrosis was the best indicator of overall shoot drought tolerance in cowpea, more so than wilting. Stem diameter was highly correlated with resistance to lodging and with both unifoliate and trifoliate necrosis, but stem diameter was not as well correlated with resistance to wilting. A unifoliate stay-green trait was discovered in some cultivars, but this trait did not co-segregate with trifoliate necrosis suggesting that it may be unrelated to drought tolerance. The goal of this research was to determine how cowpea cultivars differ in the mechanism and level of shoot drought tolerance in terms of gas exchange, carbohydrate partitioning, and leaf water content during water stress.

3.2 Materials and methods

A subset of six contrasting drought tolerant and susceptible cultivars from both the U.S. and Africa were chosen for this study (Table 3.1). One hundred twenty-six 3.8-L pots were filled volumetrically with Metro-mix® 366 planting media (Sun Gro Horticulture Canada CM Ltd., Vancouver, British Columbia, Canada) and packed to 2.5 cm from the top to allow adequate head space for watering. The media, a coarse mix of sphagnum peat moss, vermiculite, and bark has an approximate bulk density of 0.160 g cm^{-3} and is resistant to settling thereby retaining a relatively uniform water holding

capacity across the pots. Twenty-one pots were planted, one seed per pot, for each of six cultivars on a single bench in a greenhouse. The pots were arranged in a modified randomized complete block design with three replications/blocks. Each replication consisted of seven rows (one for each sampling event) of six cultivars (Table 3.1) in random order. The pots were thoroughly watered twice before planting and every three days after planting until the first trifoliate began to expand (11 days after planting). The pots received no additional water for the duration of the experiment.

Table 3.1. Cowpea cultivars evaluated for physiology of drought tolerance.

		Resistance to necrosis		
Cultivar	Source	Unifoliate	Trifoliate	Type
CB27	University of California	very resistant	very resistant	1
CB46	University of California	moderate	moderate	2
IT97K-556-4	IITA-Nigeria	moderate	moderate	2
IT99K-241-2	IITA-Nigeria	susceptible	very resistant	2
TVu-7778	IITA-Nigeria	very susceptible	very susceptible	2
TX2028-1-3-1	Texas A&M University	very resistant	very resistant	1

Measurements were taken on the 1st fully expanded trifoliate every 3-5 days until the trifoliates were chlorotic or too fragile to measure. Gas exchange measurements including photosynthesis (A_{net}), stomatal conductance (g_{sw}), transpiration (E), and intercellular CO_2 concentration (C_i) were taken in the morning (09:00-11:00 CST) using a LI-COR 6200 Portable Photosynthesis System (LI-COR Biosciences ®, Lincoln, Nebraska). The device also recorded air temperature, leaf temperature, and relative humidity, which were used to calculate the vapor pressure deficit with respect to the air

(VPD_{air}) and with respect to the leaf (VPD_{leaf}). Instantaneous water use efficiency (WUE_i) was also calculated as A_{net}/E. Before each set of measurements, the LI-COR was moved into the greenhouse and allowed to acclimate for approximately 30 minutes. The LI-COR was then calibrated using a 500-ppm CO_2 calibration gas in an air balance. For each measurement, the chamber, supported by a tripod, was clamped onto the leaf and the flow-rate through the desiccant was adjusted until the vapor pressure in the chamber stabilized. The LI-COR was configured to take two consecutive 30-second measurements. The environmental parameters for each set of measurements are shown in Table 3.2. Solar radiation was variable due to cloud cover especially on 18 days of stress when the vapor pressure in the greenhouse was substantially lower than all other measurements. Nonetheless, measurements taken on day 18 of stress continued the gas exchange trends set forth by the previous measurement events.

Table 3.2. Mean (standard deviation) of environmental conditions during gas exchange measurements of cowpea cultivars grown in a greenhouse under terminal water stress.

Days of Stress	PAR*	Air temp	Ambient CO2	Vapor Pressure
	μmol s^{-1} m^{-2}	°C	mmol CO_2 mol^{-1} H_2O	Pa
3	850 (293)	40.1 (1.7)	329 (35)	2636 (424)
7	1004 (286)	38.4 (2.6)	328 (30)	3269 (321)
10	509 (137)	35.0 (0.9)	390 (19)	2637 (156)
15	858 (503)	37.5 (2.8)	402 (14)	2862 (159)
18	369 (35)	36.1 (1.1)	408 (10)	1164 (72)

* photosynthetically active radiation (400-700 nm)

Immediately after taking gas exchange measurements, a unifoliate and a terminal leaflet from each measured plant were collected and weighed to determine fresh weight.

Each leaflet was soaked in distilled water in a petri dish for 4 hours to determine turgid weight and then oven-dried at 80°C for 24 hours to determine dry weight. The leaf moisture content (LWC) and relative moisture content (RWC) were calculated using standard formulas. The stem diameter was also measured. Each measured plant was cut off at the soil surface and approximately 200 g of soil was taken from the middle of the root zone of each pot. The plants and soil samples were dried and weighed to determine total above ground dry matter (after accounting for the leaves that were removed previously) and soil moisture content, respectively. Leaves were removed from each plant and the dry weight of the stem and petioles was recorded.

Statistical analyses were performed using SAS® 9.2 for Windows (SAS Institute Inc. Charlotte, NC). The general linear model with Tukey-Kramer means analysis was used to determine if significant differences exist between cultivars at each individual sampling interval and across all events with the event included as a fixed effect in the model.

3.3 Results and discussion

The net carbon assimilation rate (A_{net}) was highly correlated with soil moisture content, much more than stomatal conductance or transpiration (r = 0.869, 0.693, and 0.658, respectively). A_{net} was at its highest level (9.86 μmol m^{-2} s^{-1}) at the onset of the experiment when soil moisture averaged approximately 58% (g g^{-1}), but was inhibited by 15 days of stress when the soil moisture dropped below 19% (g g^{-1}) (Figures 3.1A and 3.2). A_{net} was not significantly different between cultivars at any sampling event or across all sampling events.

As soil moisture declined, intercellular CO_2 (C_i) increased steadily from 204 μmol mol^{-1} after one day of stress to 464 μmol mol^{-1} after 18 days of stress (r = -0.841; Figure 3.1D) similar to the trend Radin and Ackerson (1980) found for cotton during water stress. This resulted in a negative correlation between net photosynthesis (A_{net}) and C_i (r = -0.803; Figure 3.3) in contrast to a positive idealized A/C_i curve as is typically exhibited by plants grown under favorable conditions (Küppers et al., 1988; Flexas et al., 2006; Long and Bernacchi, 2003). Previous research has found no consistent relationship between A_{net} and C_i in cowpea under water stress. Souza et al. (2004) found a positive relationship between A_{net} and C_i in cowpeas grown under mild water stress whereas Anyia and Herzog (2003) found that C_i increased during early and moderate stress and then declined under severe stress while A_{net} declined early and remained near zero.

In this present study, the increase in C_i was partially due to an increase in ambient CO_2 concentration (from 326 to 409 μmol mol^{-1}) over the duration of the experiment. A positive correlation between C_i and C_a (r = 0.866) was expected; however, the C_i/C_a ratio was also highly, negatively correlated with A_{net} (r = -0.725). Therefore, increasing C_a only accounted for a small proportion of the negative relationship between A_{net} and C_i.

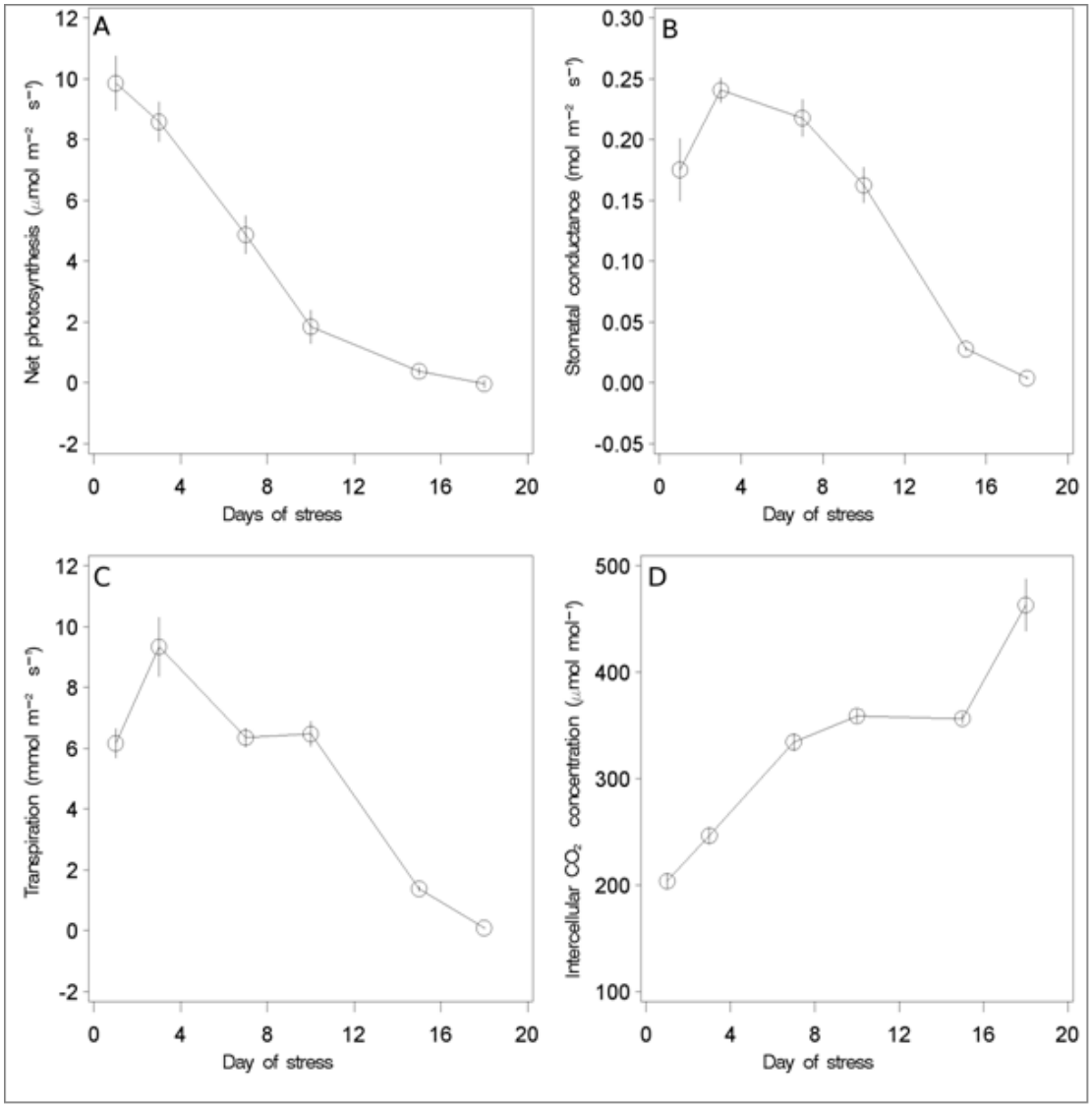

Figure 3.1. Average gas exchange measurements over time of the youngest fully-expanded trifoliate of 3 replications of 6 cowpea cultivars grown in a greenhouse under terminal water stress. A, net photosynthesis; B, stomatal conductance; C, transpiration; D, intercellular CO_2 concentration. There were no significant differences between culitvars for any of the measured traits.

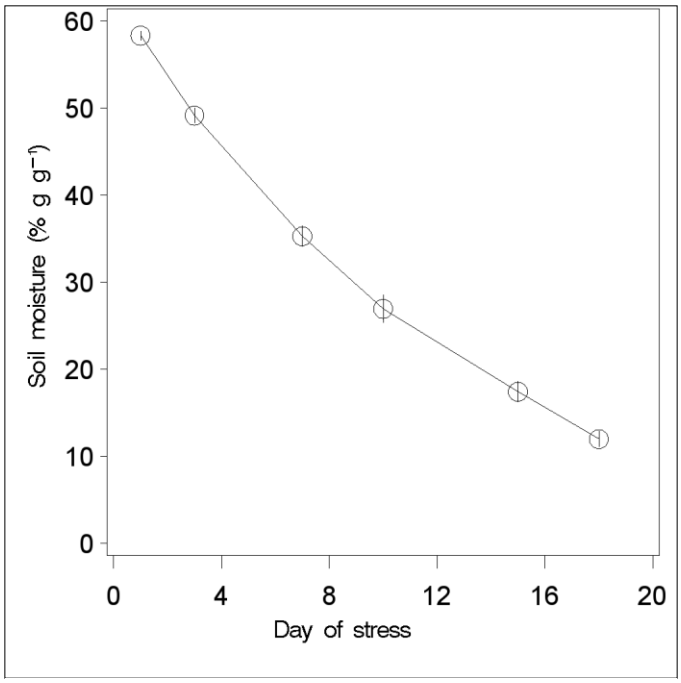

Figure 3.2. Average gravitational soil moisture content of the root zone over time of 3 replications of 6 cowpea cultivars grown in a greenhouse under terminal water stress. Each 2.5-L pot was filled with Metro-mix® 366 planting media (Sun Gro Horticulture Canada CM Ltd., Vancouver, British Columbia, Canada) which has an approximate bulk density of 0.160 g cm^{-3}.

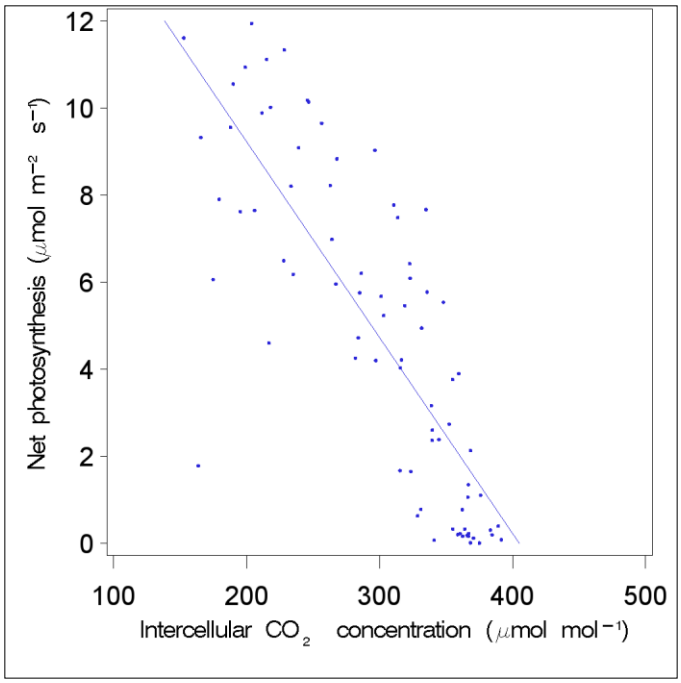

Figure 3.3. Average net photosynthesis vs. intercellular CO_2 concentration (A/C_i curve) of 3 replications of 6 cowpea cultivars on each of 6 sampling events grown in a greenhouse under terminal water stress.

Stomatal conductance and transpiration increased for most cultivars until 3 days of stress when both began to decline sharply and became approximately zero by 18 days of stress for all cultivars (Figure 3.1B and 3.1C, respectively). Peak stomatal conductance, approximately 0.25 - 0.30 mols m^{-2} s^{-1}, was not significantly different between cultivars. There were no notable differences in the start of decline, rate of decline, or point of inhibition of stomatal conductance between any cultivars. There were also no differences in instantaneous water use efficiency between cultivars at any sampling event. As expected, stomatal conductance was significantly reduced by water stress, however, it did not appear to be limiting photosynthesis or CO_2 intake as

previously suggested (Souza et al., 1982; Cornic and Briantais, 1991). Rather, the high C_i suggests a different metabolic limitation such as mesophyl conductance (Flexas et al., 2006), triose-phosphate utilization (TPU; Sharkey, 1985), or impairment or down-regulation of the photosynthetic apparatus (Shakel and Hall, 1979; Epron et al., 1992; Anyia and Herzog, 2003). However, an impairment of the photosynthetic apparatus does not explain increasing C_i even at the onset of water stress as was found in this present study and by Anyia and Herzog (2003).

Stem and petiole dry weight (Figure 3.4) and stem diameter (Table 3.3) increased significantly for all cultivars until 7 days of stress (except stem diameter in CB27). The dry weight of the youngest trifoliate (Figure 3.5) also increased significantly until 7 days of stress for all cultivars except CB27 and CB46. The dry weight of the unifoliates of drought susceptible cultivars declined until 10 days of stress whereas the dry weight of the drought tolerant ones remained constant especially for the most drought tolerant "type 1" variety, TX2028-1-3-1. By 7 days of stress, A_{net} was approximately 50% of the initial non-stressed rate, yet the unifoliates had already begun to senesce in type 2 cultivars despite increasing C_i. This shows some degree of active partitioning whereby growth of the youngest trifoliate is preserved and stems and petioles continue to increase in mass while the older unifoliates senesce. Excess photosynthate may have caused carbon assimilation to be TPU-limited (Sharkey, 1985) and carbohydrates may have been translocated from younger leaves to stems and petioles for storage during the early stages of stress as Huber et al. (1984) observed in soybean (*Glycine max*). All cultivars showed the same behavior regardless of the level or type of drought tolerance. In fact,

there were no significant differences in A_{net}, C_i, total aboveground dry matter, or total leaf dry weight between cultivars at any sampling event. However, the most drought tolerant "type 2" cultivars had larger stem diameter (Table 3.3) than the other cultivars, and significantly higher stem and petiole dry weight than two of the drought susceptible cultivars (TVu-7778 and CB27) when using a combined analysis across sampling events.

The "type 1" cultivars (TX2028-1-3-1 and CB27) had larger differences in dry weight between the unifoliates and the first trifoliates than did the susceptible cultivars (CB46 and TVu-7778). They also had significantly higher unifoliate dry weights on the last sampling event than the most susceptible cultivars (TVu-7778 and CB46) and the most drought-tolerant "type 2" cultivar (IT99K-241-2), which is consistent with the findings of Mai-Kodomi et al. (1999a). Fresh weight (Figure 3.6) and turgid weight (not shown) of the unifoliates declined in all cultivars except the most drought tolerant "type 1" and "type 2" cultivars which were steady throughout the experiment.

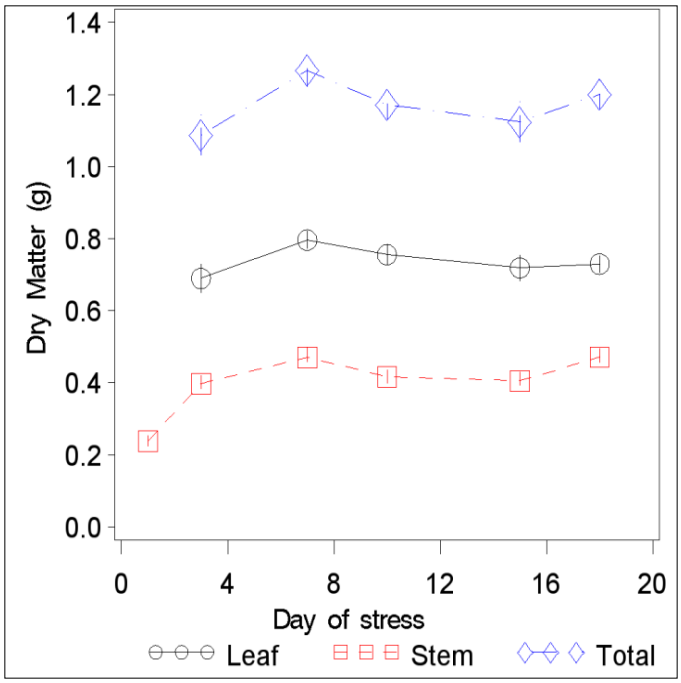

Figure 3.4. Average dry matter partitioning over time of 3 replications of 6 cowpea cultivars grown in the greenhouse under terminal water stress.

Table 3.3. Average stem diameter over time of 3 replications of 6 cowpea cultivars grown in a greenhouse under terminal water stress.

	Days of Stress									
Cultivar	3		7		10		15		18	
					mm					
CB27	3.6	a	3.7	c	3.8	a	3.4	a	3.7	b
CB46	3.7	a	4.0	bc	4.1	a	3.8	a	3.7	b
IT97K-556-4	3.6	a	4.2	ab	3.7	a	4.1	a	4.1	b
IT99K-241-2	4.5	a	4.7	a	4.5	a	4.2	a	4.8	a
TVu-7778	3.5	a	3.6	c	3.6	a	3.4	a	3.7	b
TX2028-1-3-1	3.7	a	4.1	bc	3.9	a	3.8	a	4.2	ab

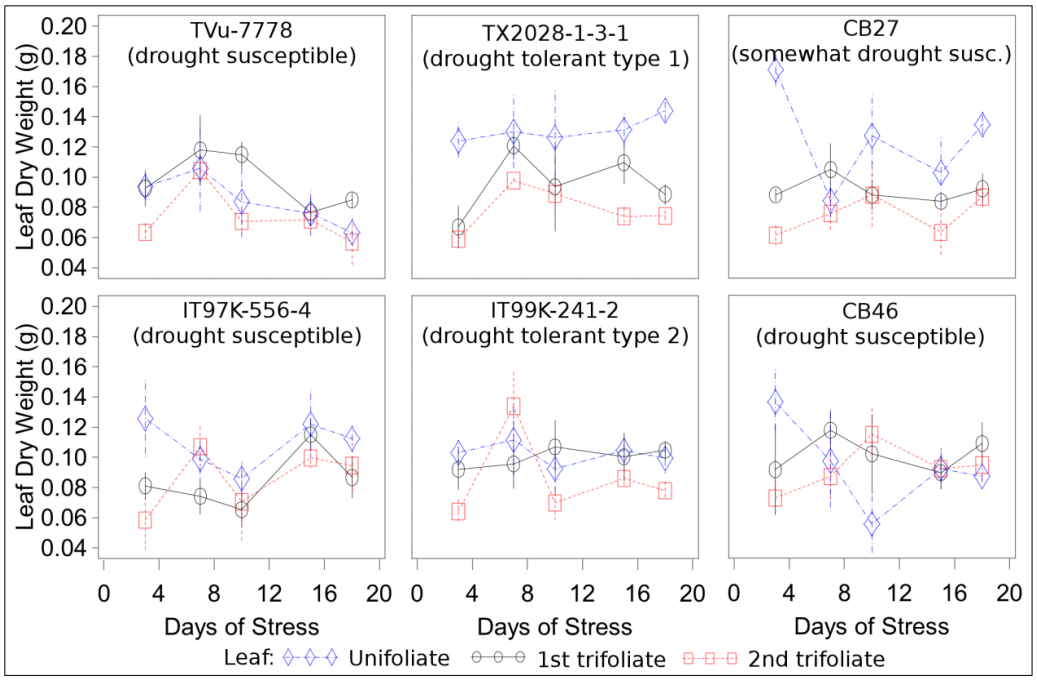

Figure 3.5. Average leaf dry weights over time of 3 replications of 6 cowpea cultivars grown in a greenhouse under terminal water stress.

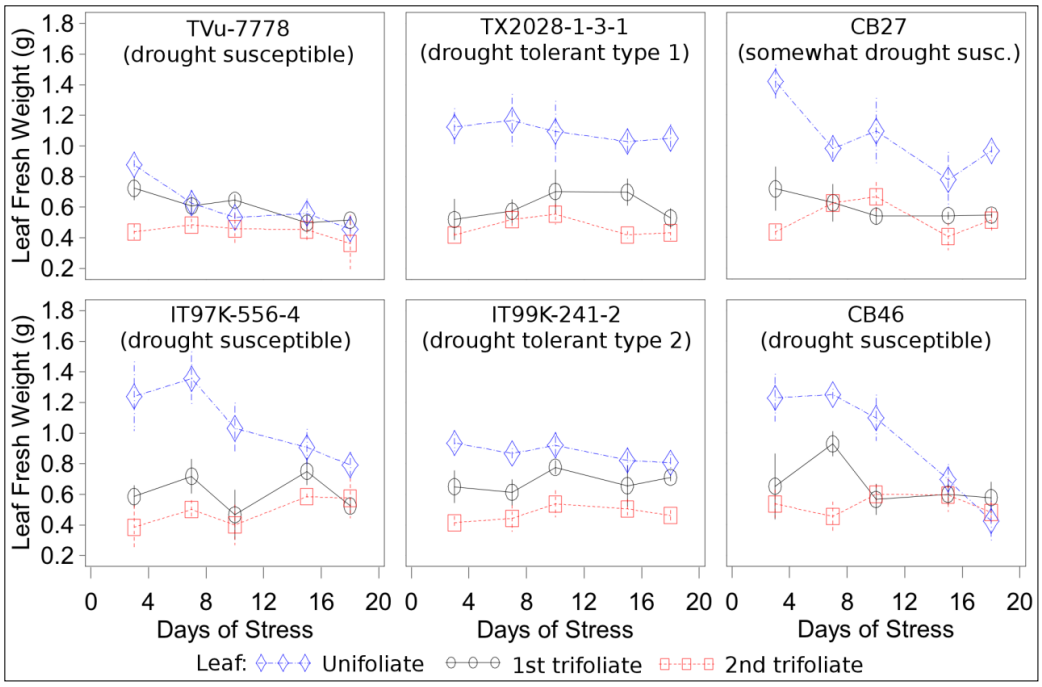

Figure 3.6. Average leaf fresh weights over time of 3 replications of 6 cowpea cultivars grown in a greenhouse under terminal water stress.

The leaf water content (LWC) (Figure 3.7) of the 1st trifoliates was well-maintained in all cultivars throughout the experiment whereas that of the unifoliates began to decline after 7 days of stress. Bates and Hall (1981) concluded that leaf water potential in cowpea was largely unaffected by treatments that differed significantly in leaf conductance. The only significant differences in LWC found between cultivars were for the unifoliates at the first and last sampling event. Pairwise differences at the first sampling event had no correspondence to the level or type of drought tolerance and were likely due to early differences in the seedling growth rate. On the last sampling event, the most "type 2" drought tolerant variety (IT99K-241-2) had significantly higher LWC in its unifoliates than a moderately susceptible variety (CB46). As expected, the LWC

was slightly higher in the unifoliates than the 1st trifoliates for all cultivars and sampling events which may correspond to a water potential gradient from root to shoot found in most species (Morgan, 1984, Teare and Kanemasu, 1972).

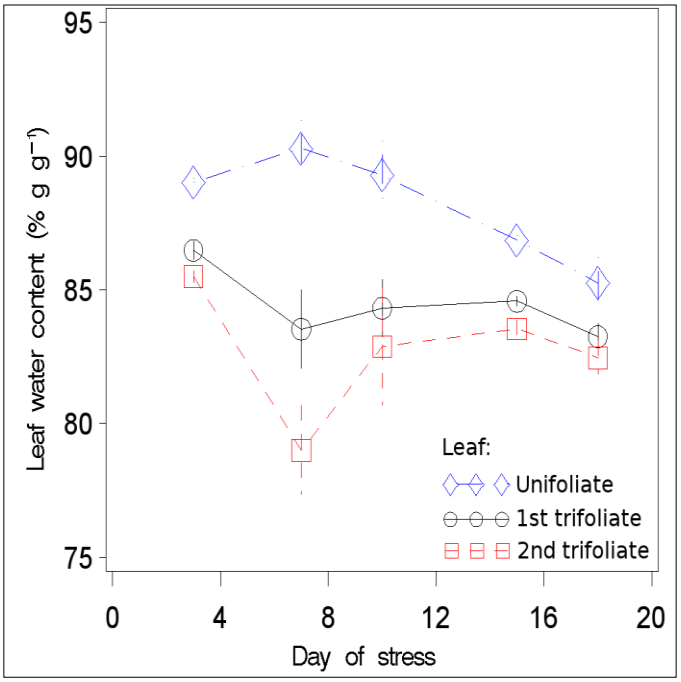

Figure 3.7. Average leaf water content over time of 3 replications of 6 cowpea cultivars grown in a greenhouse under terminal water stress.

There were no significant differences in RWC between cultivars at any event except for the severely desiccated unifoliates at and beyond 15 days of stress (Table 3.4). This was due to the inability to rehydrate the chlorotic and necrotic leaves to their full turgid weight from an apparent degradation of the cell membranes. The difference in RWC between the unifoliate and 1st trifoliate varied significantly by cultivar. All

cultivars except the most drought tolerant "type 2" (IT99K-241-2) had higher average RWC in the unifoliates than the trifoliates. The most drought tolerant "type 1" (TX2028-1-3-1) and the most drought susceptible (TVu-7778) had 7.8% and 10.5% higher RWC in the unifoliates, respectively, whereas the most drought tolerant "type 2" cultivar had 1.3% higher RWC in the 1st trifoliates. While these differences between the unifoliates and trifoliates support the findings of differential responses in cowpea to water stress reported by Mai-Kodomi et al. (1999a), there was no apparent relationship between RWC or LWC and drought tolerance. Rather, a relatively constant LWC across all cultivars suggests that the differences in RWC found between leaves of the most drought tolerant "type 1" variety were merely due to unifoliate senescence. Further, the decline in fresh weight and turgid weight was more closely correlated with declining dry weight than LWC. Therefore, this study found no evidence that the overall plant water status was significantly improved by the senescence of the unifoliates to conserve moisture in "type 2" cultivars and it appears that delayed senescence of the trifoliates may have a greater effect on conferring drought tolerance than the conservation of plant moisture. While it is unknown if delayed leaf senescence confers drought tolerance under field conditions, cultivars with genetically delayed leaf senescence have higher combined yields under favorable conditions due to multiple podsets (Gwathmey et al., 1992).

Table 3.4. Average relative water content over time of 3 replications of 6 cowpea cultivars grown in a greenhouse under terminal water stress.

	Days of Stress									
Cultivar	3		7		10		15		18	
					%					
Unifoliate										
CB27	85.8	a	88.3	a	87.9	a	87.5	ab	83.8	ab
CB46	86.8	a	86.3	a	84.6	a	80.0	b	76.1	b
IT97K-556-4	84.6	a	83.5	a	84.7	a	80.5	b	82.8	ab
IT99K-241-2	83.0	a	82.6	a	86.2	a	86.8	ab	82.8	ab
TVu-7778	87.9	a	82.2	a	88.3	a	77.8	b	95.8	a
TX2028-1-3-1	86.1	a	89.9	a	89.3	a	91.5	a	91.0	ab
1st trifoliate										
CB27	78.1	a	82.6	a	79.8	a	83.6	a	79.7	a
CB46	74.3	a	76.5	a	59.5	a	83.6	a	70.8	a
IT97K-556-4	78.7	a	85.5	a	74.2	a	84.5	a	80.1	a
IT99K-241-2	83.1	a	87.1	a	84.4	a	87.2	a	86.3	a
TVu-7778	83.0	a	85.2	a	86.0	a	82.2	a	85.7	a
TX2028-1-3-1	77.8	a	81.6	a	83.9	a	84.4	a	80.9	a
2nd trifoliate										
CB27	76.3	a	82.7	a	83.7	a	78.2	a	73.4	a
CB46	76.9	a	77.8	a	70.4	a	79.1	a	70.2	a
IT97K-556-4	74.9	a	79.3	a	64.4	a	79.2	a	83.9	a
IT99K-241-2	80.0	a	82.0	a	79.2	a	81.8	a	85.2	a
TVu-7778	77.0	a	82.0	a	82.4	a	81.8	a	82.6	a
TX2028-1-3-1	76.1	a	82.2	a	77.2	a	76.1	a	78.6	a

3.4 Conclusions

Under our experimental conditions, water stress had little effect on leaf water content, which was largely maintained and had no correspondence to the level or type of seedling drought tolerance observed in a previous experiment. Water stress did reduce net photosynthesis, stomatal conductance and transpiration of the trifoliates in all cowpea cultivars regardless of the level or mechanism of drought tolerance and no

significant differences were found between cultivars. At the same time, the intercellular CO_2 concentration increased suggesting that reduced photosynthesis was not due to the stomata limiting CO_2 availability or photorespiration. During the early stages of water stress, trifoliate photosynthesis rapidly declined and the unifoliates of susceptible cultivars began to senesce while the younger trifoliates and the stems and petioles continued to increase in weight. This suggests that excess photosynthate was being exported from the younger leaves and stored in the stems and petioles. The high intercellular CO_2 concentration in the younger leaves suggests that excess triose-phosphates may have accumulated there and inhibited photosynthesis by binding up available phosphorus. Early unifoliate senescence exhibited by certain cultivars appears to be a general stress response that does not seem to be related to drought tolerance under greenhouse conditions.

The most drought tolerant "type 2" cultivar had significantly larger stem diameter than all of the other cultivars and had significantly higher stem and petiole dry matter than more susceptible cultivars. The difference between unifoliate and trifoliate dry leaf weight was smaller for "type 1" susceptible cultivars than "type 2" cultivars. The "type 2" cultivars also had heavier unifoliates at the end of the experiment than did the most susceptible and most tolerant "type 1" cultivars. Mai-Kodomi et al. (1999a) postulated that the drought tolerance of "type 2" cultivars could be the result of a remobilization of moisture from the unifoliates to the growing tips. However, this study found no evidence that the overall plant water status was improved by the senescence of the unifoliates to conserve soil moisture in "type 2" cultivars. Fresh weight and turgid

weight of the unifoliates remained steady for the most drought tolerant cultivars regardless of type whereas it declined in susceptible cultivars. However, the decline in fresh and turgid weights of susceptible cultivars was more closely related to loss of dry weight (senescence) than to loss of moisture content.

4. THERMAL IMAGE ANALYSIS SOFTWARE FOR BREEDERS AND PHYSIOLOGISTS

4.1 Introduction

As a plant transpires, energy is absorbed by water as it is converted to vapor, thereby reducing the leaf's surface temperature. Leaf temperature can therefore be used as an indirect measurement of transpiration and is often used as an indicator of overall plant water status (Balota et al, 2007; Ehrler, 1973; Blum et al. 1982; Jackson et al. 1981; Idso, 1982). It has also been used to evaluate how a plant responds to environmental stress (Ehrler et al., 1978; Idso, 1982; Howell et al., 1986; Jackson et al. 1981) and to compare cultivars with respect to drought tolerance (Ayeneh et al., 2002; Blum, 1989; Blum et al. 1989; Pinter et al., 1990; Rashid et al., 1999; Royo et al., 2002; Reynolds et al., 1994, 2001; Fischer et al., 1998). Cooler canopy temperature is often correlated with higher yields (Amani et al., 1996; Fischer et al., 1998; Pinter et al.,1990; Rashid et al., 1999).

The use of leaf temperature or any other single trait as a selection criterion in breeding for drought tolerance is not straightforward. Leaf or canopy temperature can be significantly influenced by several plant traits including canopy color (Ferguson et al., 1973), root morphology, leaf orientation (Balota et al., 2008), leaf morphology (Balota et al., 2008; Smith, 1978), stomatal and leaf conductance, atmospheric factors including air temperature (Jackson et al., 1977), solar radiation, wind speed, and vapor pressure deficit (Jones, 1999b), and soil water availability (Blum, 1989).

The invention of low-cost infrared thermometers (IRTs) largely spurred the use of leaf temperature measurements for scientific research and breeding. For example, it has been used successfully to select for *Arabidopsis* mutants deficient in abscisic acid (ABA) signaling and ABA synthesis causing their leaf temperatures to be cooler during water stress (Merlot et al., 2002; Mustilli et al., 2002). However, IRTs have several limitations. They are typically used to take single point measurements on individual leaves. While it can also be used to take the average temperature of the canopy, they are not suitable for stressed environments with poor stands because any canopy openings may result in background soil temperature being averaged into each measurement, thus decreasing its precision (Jones, 2004; Guiliani and Flore, 2000). The utility of IRTs is also limited in the number of measurements that can be taken in a given period of time under changing environmental conditions.

Thermal imaging has been suggested as an improvement over traditional IRTs. This technology takes an instantaneous thermal image of a field of view consisting of over a hundred-thousand simultaneous discrete temperature measurements. It can greatly increase the throughput of assessing canopy temperature of a plot, trial, or field. However, it is also affected by changes in atmospheric conditions (Gonzalez-Dugo et al., 2006; Jones, 2004), background soil interference, shading (Kimes, 1980), and viewing angle (Francois et al., 1997; Kimes, 1980; Jones, 2004).

One of the most important issues for analysis of both IRT and thermal imaging data is filtering out temperature readings from the soil or any other non-target areas. This is not possible with single point IRTs, however, several attempts have been made to

filter soil out of thermal images. Guiliani and Flore (1999) used black polypropylene as a background because it has a discernibly higher temperature than plant leaves, which could then by filtered out using a threshold function. Jones et al. (2002) used wet and dry surfaces to set upper and lower thresholds as data filters. Jones and Leinonen (2003) and Leinonen and Jones (2004) later used remote sensing software to combine visual imagery and multi-spectral data with canopy temperature in order to filter out non-vegetative areas. In most cases, these techniques are "supervised" approaches in which the user must select target or non-target references areas for each thermal image so that the software can correctly distinguish which areas to filter out. Jones (2004) suggests that this is not possible with single-channel thermal images. However, given a suitable environment whereby the target area (plant material) is significantly different in temperature than the non-target area (soil), it may be possible to apply clustering algorithms to filter out the soil automatically in an unsupervised fashion.

The objective of this study was to test whether a software algorithm could be used to: 1) Automatically process a large number of thermal images and filter out non-target areas (such as soil), 2) Compute the size, mean, and other summary statistics for the target area (i.e. the plant canopy), and 3) Export the results to a file for subsequent analysis using standard statistical packages.

4.2 Software design approach

Commercial off-the-shelf thermal imaging devices are relatively inexpensive, easy to use, and often provide user-friendly software. However, these software packages are not designed with the complex filtering algorithms necessary to analyze

thermograms with heterogeneous data. Furthermore, the raw data obtained from these devices is encoded in a proprietary format within a JPEG image file (ISO/IEC IS 10918-1 | ITU-T Recommendation T.81) so that images can be readily viewed using any picture viewing software. Therefore, the following steps must be achieved in order to analyze a thermal graph:

1. Extract and decode the raw thermal data stored in a proprietary format in the JPEG image file and convert it to a public format. Currently, only the software provided by the manufacturer has this capability. For example, FLIR Systems, Inc. (Boston, MA) provides ThermalCAM Researcher 2.8 software that can open thermal image files and export the data to a new file in the "FLIR Public File Format". This file format is fully specified in the FLIR ThermaCam documentation.
2. Use custom Software to import the data.
3. Use custom Software to select a target area or areas, filter out the soil temperature data, and output results to a non-proprietary file format that any number of statistical packages can import as a comma delimited ASCII text file (comma-separated values or CSV).

4.3 Test-cases

To ensure that the Software would be capable of analyzing images taken from a range of plant species and environments, two experiments were conducted using the FLIR ThermaCam S45HS. First, thermal images were taken of winter wheat grown

under rainfed and irrigated conditions from a boom lift approximately 9m above each plot (described in Section 5). This experiment addressed the need of breeders to rank genotypes with precision under rapidly changing conditions. Second, thermal images were taken of cowpea seedlings grown in a soil box in a growth room (described in Appendix E) under water stressed conditions with the thermal camera configured to take thermal images every 30 minutes 24-hours day^{-1}. This experiment addressed the need of physiologists to investigate the mechanisms of drought tolerance by using an automated unsupervised batch processing of hundreds of thermal images.

4.4 Typical use-case scenario

The typical use-case scenario of the Software after the thermal image has been converted into a public file format is as follows:

1. Open a thermal data file
2. Draw rectangles or polygons around target areas and assign an unique identifier to each of them
3. Select plant and/or soil reference areas for automatic inversion
4. Set a threshold filter manually or check one of the automatic filtering algorithms
5. Click a button to log the filtered results to a CSV file
6. Advance to the next image in the current working directory, make adjustments as needed, and append more results to the output file
7. Alternatively, invoke a command that will automatically process all images in the current working folder using the current settings and log all results to a single CSV file

8. Optionally save selections (all points of each selected polygon and the selection identifier) to a CSV file

4.5 Filtering algorithms

Several methods of filtering-out soil were evaluated; however, the two most effective methods employed a bimodal peak detection algorithm and a two-means clustering algorithm discussed herein. The methods were evaluated visually as well as by comparison with single point IRT measurements. The suitability of these two algorithms depended largely on the environmental conditions under which the measurements were made and the variance of the soil and canopy temperatures. The two-means clustering algorithm proved the most robust when a sufficient amount of visible soil was present. In the wheat field experiment, a single thermal image consisted of two plots side-by-side with a bare 0.5-m alley in-between. The alley provided adequate visible soil such that the 2-means clustering algorithm was consistent across thermal images. The 2-means clustering approach was also successful in the cowpea experiment until the plant canopy completely covered the soil. However, the bimodal peak detection algorithm appeared to be only slightly more accurate but less robust because it required that both the soil and canopy peaks (modes) could be assessed from a frequency histogram (Figure 4.1).

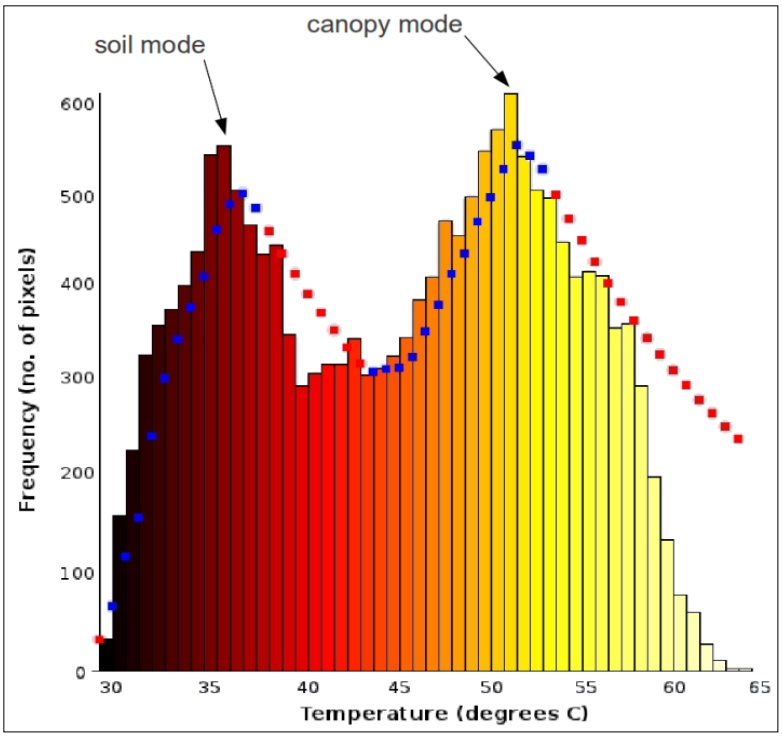

Figure 4.1. Screenshot of Software showing a bimodal canopy and soil temperature distribution of a winter wheat plot grown at the AgriLife Experiment Station at Bushland, TX in 2009.

4.5.1 Two-means clustering algorithm

The two-means clustering algorithm (Box C-1) begins with two clusters positioned at the extreme minimum and maximum temperatures of the image. Each temperature in the image is then added to the cluster with the closest mean temperature (or center). The mean temperature of each cluster is then recomputed. Once all temperatures have been assigned to the nearest cluster, the process repeats using the means of the two clusters from the current iteration as the initial centers of the clusters in the subsequent iteration. The algorithm loops until the centers of the previous iteration is within 0.005 °C of the centers of the last iteration. This occurs in approximately 6 iterations. The filtering threshold is then determined as the mid-temperature between the means of the two clusters.

The precision of the two-means clustering approach is reduced when the temperature of the soil overlaps with that of the plant material (19.5-20.4 °C in Figure 4.1). Therefore, temperature measurements should be made when the soil and canopy temperatures have the greatest separation and lowest variance. Judicious timing of measurements and irrigation can accomplish this.

4.5.2 Bimodal peak detection algorithm

The bimodal peak detection algorithm begins by dividing the temperature range of the image into approximately 50 bins (Box C-2). The exact number of bins depends on the number of temperatures measurements being assessed and the desired accuracy of the detected peaks. Each temperature reading is placed in the appropriate bin and the count in each bin is recorded. Then, the algorithm loops through the count of each bin. If

a smaller bin size is used, the curve of the frequency histogram will not be as clean. Therefore, several filters are used to "clean-up" the curve without sacrificing precision. First, a high-pass filter (Box C-3) is used to prevent spikes on the front-side of the curve from creating a false apex. Second, a low-pass filter (Box C-4) is used to prevent bins with a low number of samples from causing a false end of the peak. Lastly, a moving average filter of about 4 samples wide is applied to smooth the curve even further. Figure 4.2 shows an example of the values after applying these filters as indicated by the red dots. Once a peak is detected, a decay function (Box C-5) in conjunction with the low-pass filter is used to prevent the accidental detection of peaks on the backside slope (shown by the red dots in Figure 4.1). The number of bins, the alpha value of the high- and low-pass filters, the number of bin counts averaged for the moving average filter and the epsilon of the decay function can all be adjusted for different environments or types of vegetation.

If exactly two peaks are detected, the filter threshold is set to the mid-temperature between the two peaks. The peak temperature is the average temperature of the bin in which it is detected.

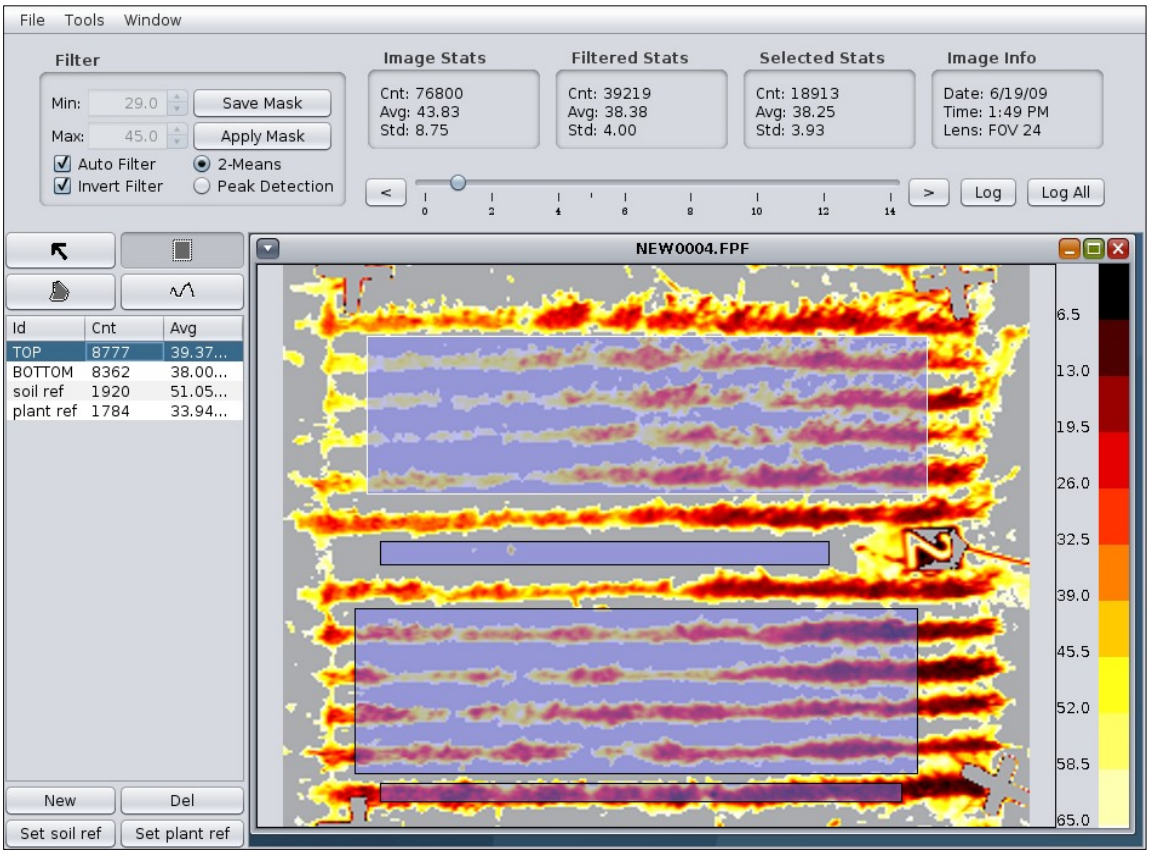

Figure 4.2. Screenshot of Software using a two-means clustering algorithm with soil and plant references to filter soil out from a winter wheat field plot. Soil and plant references have been set to automatically invert the filter as necessary.

4.5.3 Masking

Sometimes a bimodal temperature distribution cannot be detected especially during cloudy days or at night when solar radiation is low and the contrast between the soil and plant material is poor. In some species and cultivars, a bimodal distribution may not be detectable under water stress even during the day when high stomatal resistance causes the canopy temperature to be close to that of the soil. Figure 4.3 shows one such example in cowpea. After 40 days of water stress, thermal images taken at night have good contrast and a bimodal temperature distribution whereas during the daytime, one peak was detected and some cultivars and plants were warmer than the soil while others were cooler than the soil.

Therefore, the masking feature was added to the peak detection algorithm. At times when adequate contrast between the plant and soil temperature does exist and two peaks are successfully detected, the Software creates a mask of the filtered pixels. The Software then uses this mask for filtering subsequent images when two peaks cannot be successfully resolved, thereby employing the last good filter. This approach requires the thermal camera to be stationary and that the plants move little between the creation of the mask and until a bimodal distribution can once again be detected. Thus, it proved most successful for the continuous monitoring of cowpeas under growth room conditions. The user can enable and disable auto-masking and also save a mask of the current filter and apply that mask to another image manually.

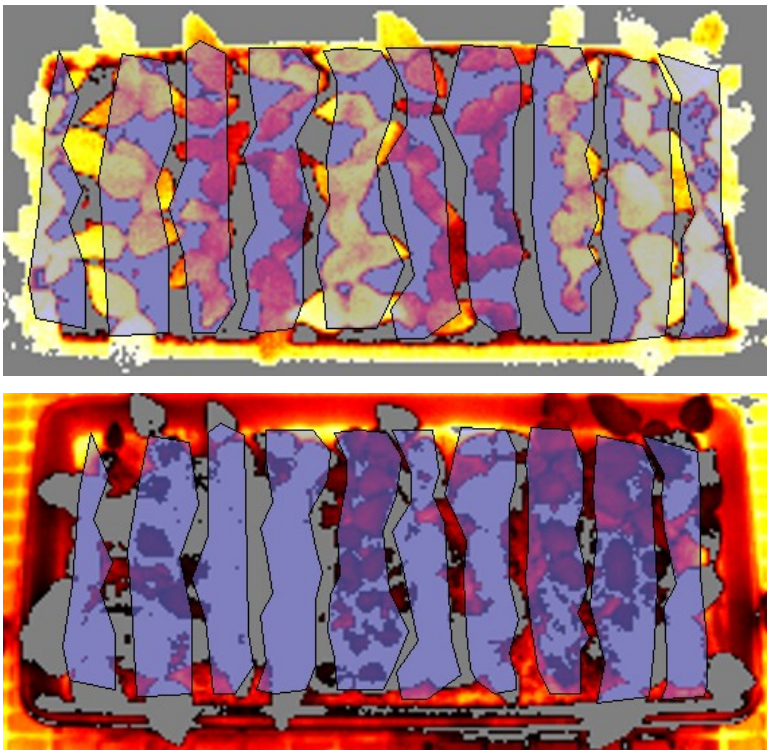

Figure 4.3. Thermal image of cowpea seedlings grown in a box in a grownroom after 40 days of water stress under dark conditions (top) and full light conditions (bottom). Both thermal images have been autofiltered using the 2-means clustering algorithm. After 40 days of water stress under full light conditions, some cultivars and plants are hotter than the soil and others are cooler than the soil.

4.5.4 Temperature inversions

Filtering the soil out of thermal images requires both a threshold value, set manually or detected by the auto-filtering algorithms, and the knowledge of whether the soil is hotter or cooler than the plant material. Additional features were added to the Software to account for temperature inversions, as is the case when the soil is cooler than the plant material. First, an option was added to allow the user to select if the soil is

hotter than the plant material. Second, plant and/or soil reference areas can be selected and designated accordingly which allows the Software to automatically determine which side of the threshold the plant material is on to properly apply the filter.

4.6 Percent ground cover

The Software records the number of filtered pixels and the number of total pixels in each selected area based on the currently selected filter. This can be used to calculate the percent of ground cover for live plant material as opposed to crop residue.

4.7 Field of view considerations

Several important factors must be considered in purchasing a thermal imaging device and in designing experiments that employ them. The most important design constraints are the field of view (FOV) of the lens or the size of area that can fit within a single thermal image and the instantaneous field of view (IFOV) or pixel size in each image. For wheat which has a small leaf width, it is preferable to have a IFOV of less than 1/2 the width of the flag leaf to avoid edge effects, when a reading along the margin of the leaf encompasses both the temperature of the plant material and also that of the background (possibly soil). These leaf and background temperatures are then optically averaged. If the IFOV is too large (greater than the width of the flag leaf in wheat), a majority of the temperature readings are averaged with some amount of background temperature. This increases the variance of the plant material as well as the overlap between the perceived plant and soil material. Background temperature will usually be

that of other leaves if the canopy is dense. However, in poor stands, the background temperature is often that of soil.

Once an IFOV has been chosen, the horizontal and vertical FOVs can be calculated by multiplying the IFOV by the dimensions of the thermal imager's focal plane array. For example, a thermal imager with a 320 x 240 focal plane array can only image a maximum area of 1.6 m x 1.2 m to achieve an IFOV of 5 mm. The FOV can then be used to determine what lens is required and how far the thermal imaging device needs to be from the target using Equation 4.1. For example, the FLIR ThermaCam S45HS comes with a 36 mm lens with a θ_{lens} of 19.1°. Using the maximum FOV dimension (1.6 m), it was determined that the device needed to be about 4.8 m above the target plot. However, a compromise was made to use a slightly higher IFOV in order to capture the width of two adjacent wheat plots, thereby sacrificing some precision.

$$d = \frac{\mathrm{FOV}/2}{\tan\left(\theta_{lens}/2\right)} \qquad (4.1)$$

4.8 Data output

The user can log an analysis of selected areas to a file using two methods. The "Log" button analyzes the selected areas of the current image using the currently selected filter and writes the results to a file. The "Log All" button loops through all images in the current working directory, analyzes the selected areas of each image using

the currently selected filter, and writes the results of each image to a file. If an auto-filtering algorithm is selected, the Software runs the auto-filtering algorithm separately for each image; otherwise, the current manual filter is used for all images.

Data is logged to a CSV file with columns defined in Table 4.1. The first time that the user chooses to log data to a file, a dialog is displayed allowing the user to select the output file and directory. Subsequent logging actions will append the data to the previously selected file.

Table 4.1. Output log file format of Software for post-processing thermal images.

Column	Field Description
1	time of the thermalgraph in the format of HH:MM:SS
2	decimal day of year of the thermalgraph
3	selection ID, assigned by the user
4	number of selected filtered pixels
5	total number of selected pixels (unfiltered)
6	minimum temperature of the threshold filter (set by user or set automatically by the autofiltering algorithm)
7	maximum temperature of the threshold filter (set by user or set automatically by the autofiltering algorithm)
8	mean temperature in Celsius of the selected filtered pixels
9	standard deviation of the mean temperature of the selected filtered pixels
10	minimum temperature in Celsius of the selected filtered pixels
11	maximum temperature in Celsius of the selected filtered pixels
12	number of selected filtered pixels for an inverted threshold
13	mean temperature in Celsius of the selected filtered pixels when the threshold is inverted. This can also be used as the average temperature of the background soil on a non-inverted filter.

4.9 Software specifications

The Software was written in Java™ using the Sun Java Platform, Standard Edition 6 Development Kit (version 1.6.0 29). Therefore, it requires a separate installation of the Sun Java Runtime Environment (JRE) version 6 or greater to run which can be downloaded from the Oracle website: http://www.oracle.com/technetwork/java/javase/downloads. Earlier versions of the runtime may work but they have not been tested and are not officially supported. The Software runs on any platform and operating system for which there is a suitable Java runtime installed.

Aside from the installation requirements of the Java runtime, the Software requires approximately 3 MB of free disk space to install and about 2x the size of the largest image file that is to be loaded in free memory space.

4.10 Documentation

Installation instructions and the user manual can be found on the following website:

http://verbree.info/twiki/bin/view/Software/IRCropStressImageProcessor.

4.11 Availability

The Software will soon be made available for a nominal fee from the corresponding author. However, licensing and terms of availability are subject to change.

4.12 Conclusions

The Software has proved invaluable for the analysis of hundreds of thermal images in two separate studies. The two-means filtering algorithm was found to be highly robust and adaptable to many environments. However, it depends on a sufficient amount of visible soil in each image. On the other hand, in cases with a low amount of visible soil, no filtering is necessary. The peak-detection algorithm with masking also proved useful for batch processing of images with a stationary thermal imaging device and little leaf movement. Nonetheless, additional research could greatly improve this algorithm's performance by determining the optimal bin size and parameters for the filter and decay functions. Both filtering algorithms rely on good contrast between the soil and canopy temperatures and a low variance of each.

5. THERMAL IMAGING FOR HIGH THROUGHPUT PHENOTYPING OF CANOPY TEMPERATURE IN WINTER WHEAT

5.1 Introduction

Field phenotyping has the practical advantage of allowing breeders to correlate canopy temperature measurements with actual yield data. The expectation is that canopy temperature depression can be used as an indicator of drought tolerance in winter wheat. However, canopy temperature measurements are affected by changes in atmospheric conditions (Gonzalez-Dugo et al., 2006; Jones, 2004). Several attempts have been made to account for changing atmospheric conditions during measurements of canopy temperature. Jackson et al. (1977) subtracted air temperature to produce a measurement of canopy temperature depression (CTD). However, this did not account for differences in humidity and vapor pressure deficit over the course of the day or between environments. The crop water stress index (CWSI) was developed to account for humidity by using a formula that included the temperature of a well-watered reference plant or plot (Idso, 1982; Idso et al., 1982; Jackson et al., 1981). Jones et al. (1996) extended the CWSI model further by using both a wet and a dry reference to normalize measurements between environments; however, this approach still has the same temporal limitation of single-point IRTs as do other measurements. Conditions in the field can rapidly change between the measurement of the reference plant or plot and the measurement of the target plant or plot. For the purpose of ranking genotypes within a given environment, a simple alternative is to compare the adjusted means of the canopy

temperature with vapor pressure deficit included in the model as a covariate. This approach accounts for the effects of temperature and humidity on evapotranspiration from the leaf's surface. The canopy temperature rankings can then be compared with yield rankings between environments.

The objective of this study was to compare canopy temperatures and CTD of winter wheat cultivars grown under rainfed and irrigated conditions using an IRT and a thermal camera (TCAM) with a narrow- and wide-angle lens and to evaluate the relationship between canopy temperature and yield.

5.2 Materials and methods

Thermal images and IRT measurements were taken of plots of 10 hard red winter wheat cultivars (Table 5.1) in irrigated and rainfed regimes at the Texas Agricultural Experiment Station in Bushland, Texas in 2009 and 2011. No measurements were taken in 2010 due to excessive rainfall. The irrigated field was flood-irrigated with approximately 300 mm and 380 mm of water in 2009 and 2011, respectively. High temperatures and very low precipitation caused the wheat to be especially stressed on the rainfed field in 2011 (Table 5.2). Most of the cultivars were closely related and well-adapted to the high plains region. Plots were arranged in a randomized complete block design with three blocks/replications of 10 cultivars planted 6 rows per plot with 20 cm between rows. All measurements were taken approximately at anthesis. In 2009, measurements were taken of both regimes in the morning (900-1100) and in the afternoon (1300-1500) as suggested by Balota et al. (2007) to be the optimal times to measure CTD in that environmental. In 2011, measurements were taken of the irrigated

and rainfed regimes in the morning and afternoon, respectively. Thermal images were taken with a FLIR ThermaCam (model HS45S) from a 30-m boom lift 8.5 m above the plots (Figure 5.1). A weighted string was attached to the basket of the lift to ensure a precise distance between the camera and the canopy. In 2009 and 2011, a 36 mm lens (19.1° FOV; TCAM-N) was used to image two plots at a time (Figure 5.2) and a 9 mm (68° FOV; TCAM-W) was used to image five plots at a time in 2011. IRT measurements were also taken at eye-level using a Telatemp Infrared Thermometer model AG-42 D (Teletemp Corporation, Fullerton, CA) in 2009 and with an Everest Agri-Therm II (Everest Interscience Inc., Tucson, AZ) in 2011. The thermal images were post-processed using custom software (Section 4) to filter out background soil and to calculate the canopy temperature mean and standard deviation of each plot.

Table 5.1. Winter wheat cultivars planted under rainfed and irrigation regimes in 2008-2009 and 2010-2011 growing seasons in Bushland, TX.

Cultivar	Pedigree	Source/Breeder	Release Date
TAM 105	short wheat/Scout	Texas AgriLife	1979
TAM 110	TAM 107 (sib) (=TAM 105*4/Amigo)'*5//Largo	Texas AgriLife	1996
TAM 111	TAM 107//TX78V3620/CTK78/3/TX87V1233	Texas AgriLife	2002
TAM 112	U1254-7-9-2-1/TAM 110 (sib)	Texas AgriLife	2005
Dumas	WI90-425/WI89-483	AgriPro Wheat	2000
Jagalene	Jagger/Abilene	AgriPro Wheat	2002
TX99A0153-1	Ogallala/TAM 202	Texas AgriLife	(experimental)
TX86A5606	TAM 107 (sib) (=TAM 105*4/Amigo)'*5//Largo	Texas AgriLife	(experimental)
TX88A6880	TAM 107 (sib) (=TAM 105*4/Amigo)'*5//Largo	Texas AgriLife	(experimental)
TX86A8072	TAM 107 (sib) (=TAM 105*4/Amigo)'*5//Largo	Texas AgriLife	(experimental)

Table 5.2. Summary of temperature and precipitation for the 2008-2009 and 2010-2011 winter wheat growing season at Bushland, TX.

	2008-2009			2010-2011		
		Mean temperature			Mean temperature	
Month	Rainfall	Maximum	Minimum	Rainfall	Maximum	Minimum
	mm	°C	°C	mm	°C	°C
September	13	26.1	11.1	1	30.4	14.0
October	103	21.4	5.7	1	23.7	6.7
November	2	16.5	0.2	8	16.0	-1.9
December	1	12.1	-5.5	4	12.8	-3.3
January	0	12.3	-6.1	0	10.7	-8.0
February	11	16.4	-2.8	3	10.6	-7.7
March	4	18.6	0.2	16	19.0	0.4
April	26	20.9	3.8	0	24.5	4.4
May	12	24.9	9.5	1	27.7	7.9
June	61	31.3	15.4	6	35.6	16.8
Total	234			39		

Figure 5.1. Thermal imaging of winter wheat plots using a boom-lift and on the ground using an infra-red thermometerin Bushland, TX in 2009.

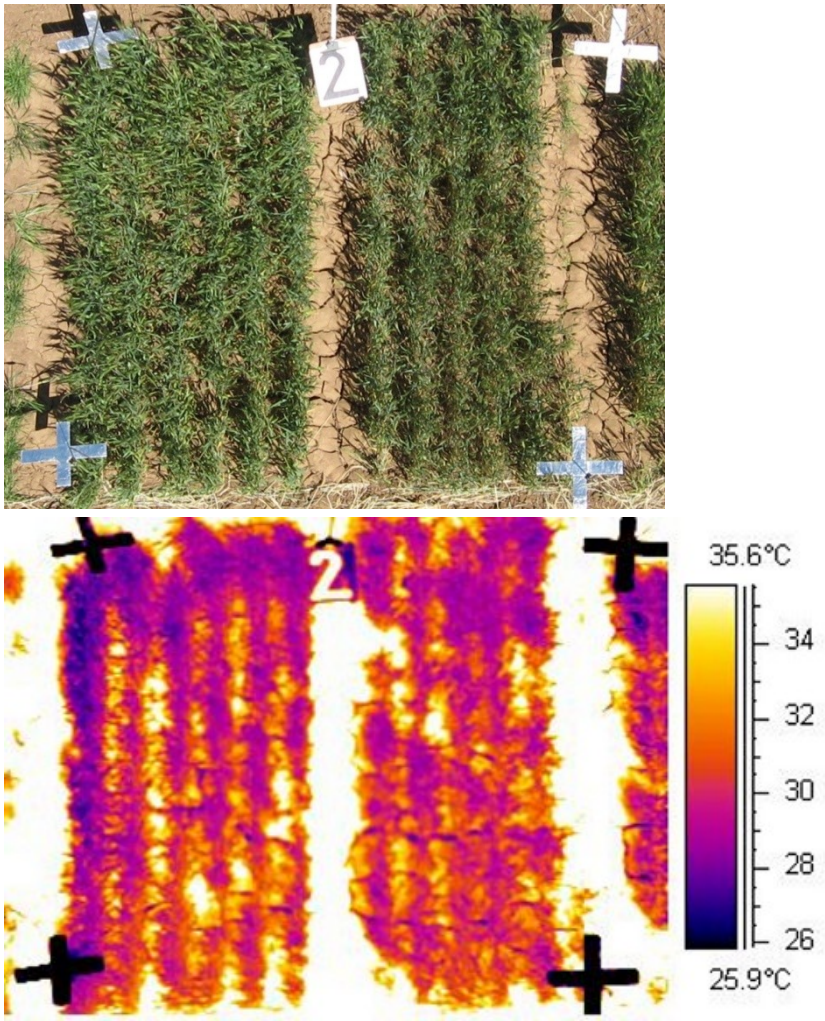

Figure 5.2. Visual image (top) and corresponding thermal image (bottom) of two winter wheat plots side-by-side in the irrigated field in Bushland, TX in 2009.

Weather data (15-min resolution) was obtained from the USDA-ARS research weather station nearby the field plots and interpolated precisely to the timestamps of each thermal image. CTD was calculated by subtracting canopy temperature (CT) from the interpolated air temperature from the weather station data. The general linear model with a Tukey-Kramer analysis was used to compare cultivars with respect to CT and CTD for each year individually and as a combined analysis across years. The CT (inverted) and CTD rankings of the ten cultivars were compared against their corresponding yield rankings in each regime for each method of measuring canopy temperature. A low average rank-shift indicates a closer relationship with yield for a given method. All statistical analyses were performed using SAS® 9.2 for Windows (SAS Institute Inc. Charlotte, NC). Pairwise comparisons between cultivars were performed using Tukey-Kramer means analysis.

5.3 Results and discussion

Vapor pressure deficit (VPD), wind speed, and block were significant covariates across all measurements for both CT and CTD as response variables. The ranking order of the adjusted means of CT and CTD of all cultivars using all methods of measurement were identical (Tables 5.3 and 5.4) when VPD and wind speed were used as covariates. This suggests that, at least for conditions similar to ours, calculating CTD from air temperature (as per Jackson et al., 1977) may be unnecessary when ranking cultivars by adjusted means if these covariates are included in the model. Further, the effect of measurement set (morning or afternoon) was no longer significant when VPD was included in the model. Indeed, Balota et al. (2007) found that these times of

measurement (900 and 1300) were quite similar due to the diurnal trend during May for that location. Therefore, VPD and wind speed were used as covariates in all analysis in order to pool morning and afternoon observations and all results are reported as adjusted means.

Under rainfed conditions, TAM110 had significantly higher yields than TX86A8072, TX86A5606, Dumas, and TAM105 in a combined analysis across years (Table 5.5) and significantly higher yields than TAM105 in 2011. Under irrigated conditions, TAM111 had significantly higher yield than TX86A8072 in a combined analysis and significantly higher yields than TX86A5606 and TX86A8072 in 2009. TAM111 had the lowest rank-shift in yield between regimes (Table 5.6) which suggests that it is both drought tolerant and responsive to irrigation. TAM110 and TAM105 had the highest rank-shift in yield between regimes. TAM110, which ranked first under rainfed conditions, ranked 8th under irrigated conditions and therefore appears to be drought tolerant but less responsive to irrigation. TAM105, which ranked last under rainfed conditions and 3rd under irrigated conditions, appears to be susceptible to drought and responsive to irrigation. TAM112 responded similarly to its close relative TAM110.

Table 5.3. Average canopy temperature at anthesis of 3 replications of winter wheat cultivars measured by infrared thermometer (IRT), thermal camera with narrow-angle lens (TCAM-N), and thermal camera with wide-angle lens (TCAM-W) grown under rainfed and irrigated regimes in Bushland, TX in 2009 and 2011.

	2009						2011									Combined				
	IRT			TCAM-N			IRT			TCAM-N			TCAM-W			IRT			TCAM-N		
Cultivar	Adj. Mean		Rank	Adj. Mean		Rank	Adj. Mean		Rank	Adj. Mean		Rank	Adj. Mean		Rank	Adj. Mean		Rank	Adj. Mean		Rank
	°C			°C			°C			°C			°C			°C			°C		
Rainfed																				
Dumas	29.2	a	3	36.1	a	7	33.7	a	4	39.9	a	6	40.8	a	5	32.2	ab	3	38.6	a	8
Jagalene	30.3	a	7	36.0	a	6	34.1	a	5	39.1	a	2	41.7	a	10	33.0	ab	6	38.1	a	2
TAM105	29.4	a	4	35.6	a	1	36.3	a	10	40.2	a	7	40.5	a	3	32.7	ab	5	38.0	a	1
TAM110	29.7	a	6	35.7	a	3	35.3	a	8	40.5	a	9	40.0	a	2	32.4	ab	4	38.1	a	4
TAM111	29.1	a	2	35.7	a	2	33.1	a	2	39.7	a	4	39.9	a	1	31.6	ab	2	38.1	a	3
TAM112	30.6	a	8	36.6	a	10	35.2	a	6	40.6	a	10	40.9	a	7	33.2	ab	9	39.0	a	10
TX86A5606	31.2	a	10	35.8	a	4	35.3	a	7	40.3	a	8	41.1	a	9	33.8	a	10	38.4	a	7
TX86A8072	30.8	a	9	36.5	a	8	33.3	a	3	38.8	a	1	40.6	a	4	33.0	ab	7	38.4	a	6
TX88A6880	29.5	a	5	35.8	a	5	35.8	a	9	39.4	a	3	41.1	a	8	33.1	ab	8	38.1	a	5
TX99A0153-1	29.1	a	1	36.5	a	9	31.3	a	1	39.8	a	5	40.8	a	6	31.1	b	1	38.8	a	9
Mean	29.9			36.0			34.3			39.8			40.7			32.6			38.4		
Irrigated																				
Dumas	21.9	a	5	25.5	ab	2	17.4	a	10	14.6	a	7	14.9	a	7	19.9	a	9	20.7	ab	2
Jagalene	21.7	a	3	26.6	ab	8	16.4	a	1	14.0	a	2	14.7	a	3	19.2	a	1	21.3	ab	6
TAM105	22.0	a	7	26.1	ab	4	16.6	a	3	14.4	a	3	15.2	a	10	19.5	a	4	21.0	ab	4
TAM110	21.8	a	4	26.3	ab	6	16.6	a	2	14.4	a	4	14.8	a	6	19.3	a	2	21.2	ab	5
TAM111	21.6	a	2	25.3	b	1	16.7	a	4	14.4	a	5	15.1	a	9	19.3	a	3	20.5	b	1
TAM112	21.9	a	6	25.9	ab	3	17.4	a	9	14.9	a	9	14.6	a	1	19.9	a	7	21.0	ab	3
TX86A5606	21.6	a	1	27.1	a	10	17.0	a	6	15.3	a	10	14.9	a	8	19.5	a	5	21.9	a	10
TX86A8072	22.0	a	9	26.8	ab	9	17.3	a	8	14.6	a	6	14.7	a	4	19.9	a	10	21.5	ab	9
TX88A6880	22.1	a	10	26.2	ab	5	17.1	a	7	14.8	a	8	14.8	a	5	19.9	a	8	21.3	ab	8
TX99A0153-1	22.0	a	8	26.6	ab	7	16.7	a	5	13.9	a	1	14.7	a	2	19.6	a	6	21.3	ab	7
Mean	21.9			26.2			16.9			14.5			14.8			19.6			21.2		

Table 5.4. Average canopy temperature depression at anthesis of 3 replications of winter wheat cultivars measured by infrared thermometer (IRT), thermal camera with narrow-angle lens (TCAM-N), and thermal camera with wide-angle lens (TCAM-W) grown under rainfed and irrigated regimes in Bushland, TX in 2009 and 2011.

	2009						2011									Combined				
	IRT			TCAM-N			IRT			TCAM-N			TCAM-W			IRT			TCAM-N		
Cultivar	Adj. CTD		Rank	Adj. CTD		Rank	Adj. CTD		Rank	Adj. CTD		Rank	Adj. CTD		Rank	Adj. CTD		Rank	Adj. CTD		Rank
	°C			°C			°C			°C			°C			°C			°C		
Rainfed																				
Dumas	-3.0	a	3	-9.9	a	7	-12.8	a	4	-19.0	a	6	-19.7	a	5	-8.6	ab	3	-14.9	a	8
Jagalene	-4.1	a	7	-9.8	a	6	-13.2	a	5	-18.2	a	2	-20.6	a	10	-9.3	ab	6	-14.4	a	2
TAM105	-3.2	a	4	-9.4	a	1	-15.5	a	10	-19.4	a	7	-19.4	a	3	-9.0	ab	5	-14.4	a	1
TAM110	-3.5	a	6	-9.5	a	3	-14.5	a	8	-19.6	a	9	-19.0	a	2	-8.7	ab	4	-14.5	a	5
TAM111	-2.9	a	2	-9.5	a	2	-12.2	a	2	-18.8	a	4	-18.8	a	1	-8.0	ab	2	-14.5	a	3
TAM112	-4.4	a	8	-10.4	a	10	-14.3	a	6	-19.7	a	10	-19.9	a	7	-9.6	ab	9	-15.3	a	10
TX86A5606	-4.9	a	10	-9.6	a	4	-14.4	a	7	-19.4	a	8	-20.0	a	9	-10.1	b	10	-14.7	a	7
TX86A8072	-4.5	a	9	-10.3	a	9	-12.5	a	3	-18.0	a	1	-19.5	a	4	-9.3	ab	7	-14.7	a	6
TX88A6880	-3.3	a	5	-9.6	a	5	-15.0	a	9	-18.6	a	3	-20.0	a	8	-9.4	ab	8	-14.5	a	4
TX99A0153-1	-2.9	a	1	-10.3	a	8	-10.5	a	1	-19.0	a	5	-19.8	a	6	-7.5	a	1	-15.1	a	9
Mean	-3.7			-9.8			-13.5			-19.0			-19.7			-9.0			-14.7		
Irrigated																				
Dumas	-2.3	a	5	-1.5	ab	2	-0.6	a	10	2.2	a	7	2.0	a	7	-1.5	a	9	0.3	ab	2
Jagalene	-2.1	a	3	-2.6	ab	7	0.4	a	1	2.9	a	2	2.2	a	3	-0.9	a	1	-0.3	ab	6
TAM105	-2.4	a	7	-2.1	ab	4	0.2	a	3	2.4	a	4	1.6	a	10	-1.1	a	4	-0.1	ab	4
TAM110	-2.2	a	4	-2.3	ab	6	0.3	a	2	2.4	a	5	2.1	a	6	-1.0	a	2	-0.2	ab	5
TAM111	-2.1	a	2	-1.3	a	1	0.2	a	4	2.5	a	3	1.8	a	9	-1.0	a	3	0.5	a	1
TAM112	-2.3	a	6	-1.9	ab	3	-0.5	a	9	2.0	a	9	2.3	a	1	-1.5	a	7	0.0	ab	3
TX86A5606	-2.1	a	1	-3.0	b	10	-0.1	a	6	1.6	a	10	2.0	a	8	-1.2	a	5	-0.9	b	10
TX86A8072	-2.5	a	9	-2.8	ab	9	-0.5	a	8	2.3	a	6	2.2	a	4	-1.5	a	10	-0.5	ab	9
TX88A6880	-2.6	a	10	-2.2	ab	5	-0.3	a	7	2.1	a	8	2.1	a	5	-1.5	a	8	-0.3	ab	7
TX99A0153-1	-2.5	a	8	-2.6	ab	8	0.1	a	5	2.9	a	1	2.2	a	2	-1.2	a	6	-0.3	ab	8
Mean	-2.3			-2.2			-0.1			2.3			2.0			-1.2			-0.2		

Table 5.5. Average yields of 3 replications of winter wheat cultivars grown under rainfed and irrigated regimes in Bushland, TX in 2009 and 2011.

Cultivar	2009 yield			2011 yield			Combined yield		
	g m^{-2}		rank	g m^{-2}		rank	g m^{-2}		rank
Rainfed									
Dumas	142	A	5	58	ab	9	99	b	9
Jagalene	142	A	4	66	ab	6	104	ab	4
TAM105	136	A	8	47	b	10	91	b	10
TAM110	160	A	1	76	a	1	117	a	1
TAM111	142	A	6	70	ab	3	106	ab	2
TAM112	144	A	3	68	ab	4	106	ab	3
TX86A5606	134	A	9	65	ab	7	100	b	8
TX86A8072	124	A	10	73	ab	2	100	b	7
TX88A6880	137	A	7	67	ab	5	103	ab	6
TX99A0153-1	148	a	2	62	ab	8	104	ab	5
Mean	141			65			103		
Irrigated									
Dumas	262	ab	7	296	a	3	279	ab	5
Jagalene	291	ab	3	291	a	6	291	ab	4
TAM105	261	ab	8	327	a	1	294	ab	3
TAM110	274	ab	6	281	a	7	278	ab	8
TAM111	332	a	1	292	a	4	312	a	1
TAM112	283	ab	4	273	a	9	278	ab	7
TX86A5606	248	b	9	292	a	5	270	ab	9
TX86A8072	233	b	10	252	a	10	243	b	10
TX88A6880	278	ab	5	277	a	8	279	ab	6
TX99A0153-1	300	ab	2	298	a	2	299	ab	2
Mean	276			288			282		

Table 5.6. Yield ranks and rank-shift between winter wheat cultivars grown under rainfed and irrigated regimes in Bushland, TX in 2009 and 2011.

	2009 yields			2011 yields			Combined yields		
Cultivar	Rainfed	Irrigated	Rank-shift	Rainfed	Irrigated	Rank-shift	Rainfed	Irrigated	Rank-shift
Dumas	5	7	2	9	3	6	9	5	4
Jagalene	4	3	1	6	6	0	4	4	0
TAM105	8	8	0	10	1	9	10	3	7
TAM110	1	6	5	1	7	6	1	8	7
TAM111	6	1	5	3	4	1	2	1	1
TAM112	3	4	1	4	9	5	3	7	4
TX86A5606	9	9	0	7	5	2	8	9	1
TX86A8072	10	10	0	2	10	8	7	10	3
TX88A6880	7	5	2	5	8	3	6	6	0
TX99A0153-1	2	2	0	8	2	6	5	2	3

Yields were highly and significantly correlated to CTD measured by both the IRT and the TCAM-N under the rainfed conditions (Table 5.7) but not under irrigated conditions. Reynolds et al. (1994) and Fischer et al. (1998) found much better correlations between yield and CTD of 16 and 8 cultivars grown under irrigated conditions ($r = 0.82$ and 0.76, respectively). However, they used more diverse varieties that had a wider range in yields than the closely-related high-plains-adapted cultivars evaluated in this present study. The TCAM-W method showed poor and inconsistent results most likely because the wide-angle lens increased the instantaneous field of view (IFOV, or pixel size) from 8.9 mm to 35.8 mm, which greatly exceeded the width of the flag leaf and therefore caused a substantial amount of background interference on poor stands. In addition, precision was reduced because only one set of measurements were taken in each regime in 2011.

In 2009, the IRT canopy temperature measurements were significantly lower than the TCAM-N measurements on both fields. In 2011, the IRT canopy temperature measurements were significantly lower than those taken by TCAM-N and TCAM-W on the rainfed field in the afternoon but significantly higher than those taken on the irrigated field in the morning. On the irrigated field, the IRT measurements taken in the morning averaged only 0.06 degrees warmer than air temperature, which was expected when solar radiation, transpiration, and evaporative cooling are lowest. However, measurements taken by the TCAM at the same time averaged 2.35 degrees cooler than air temperature. This could be the result of a high-degree of shading among plants during the morning hours. During this time, the TCAM directly above the plot captured a

greater amount of shaded plant area than the IRT that is taken at a 45-degree angle at eye-level. Conversely, when the sun is directly overhead in the afternoon, there is almost no shading visible from the point-of-view of the TCAM overhead. Similarly, Kimes et al. (1980) found that canopy temperatures varied by up to 13°C with changes in the viewing angle. Therefore, this study must be considered as a comparison of the entire methodology (height, angle, and timing of measurements) rather than just a comparison between the IRT and TCAM devices.

Table 5.7. Correlations between yield and canopy temperature depression at anthesis measured by infrared thermometer (IRT) and thermal camera with narrow-angle lens (TCAM-N) in 2009 and 2011, and thermal camera with wide-angle lens (TCAM-W) in 2011 of winter wheat grown under rainfed and irrigated regimes in Bushland, TX.

	Method		
Correlation with yield	IRT	TCAM-N	TCAM-W*
Rainfed			
Pearson correlation	0.885	0.886	0.175
P-value	<0.0001	<0.0001	0.2813
No. observations	100	100	40
Irrigated			
Pearson correlation	0.161	0.236	-0.062
P-value	0.2682	0.0263	0.7476
	49	87	29
Combined			
Pearson correlation	0.794	0.924	0.971
P-value	<0.0001	<0.0001	<0.0001
No. observations	149	186	69

* TCAM-W had only one year of data (2011) with 4 replications on the rainfed field and 3 replications on the irrigated field

The only significant difference in canopy temperature on the rainfed field was found in a combined analysis across years using the IRT whereby the canopy of TX86A5606 was significantly warmer than TX99A0153-1 (Table 5.3). TX86A5606 was also the warmest variety on the irrigated field as determined by the TCAM-N in 2009 and in a combined analysis across years. It was ranked among the lowest yielding cultivars in both environments (Table 5.5). However, it was not significantly different from any other cultivar in percent ground cover (Table 5.8) under rainfed conditions. The reason for the high canopy temperatures and low yields of TX86A5606 warrants further investigation. In the irrigated field, TAM111 had a significantly cooler canopy than TX86A5606 in 2009 and in a combined analysis when measured using the TCAM-N. It was also ranked coolest overall using the same method.

Table 5.8. Average percent ground cover at anthesis of 3 replications of winter wheat cultivars grown under rainfed conditions in Bushland, TX in 2009 and 2011.

Cultivar	2009 cover			2011 cover			Combined cover		
	%		rank	%		rank	%		rank
Dumas	50.9	a	6	42.3	a	6	46.7	a	7
Jagalene	56.0	a	3	40.2	a	9	47.7	a	5
TAM105	50.9	a	7	39.0	a	10	44.8	a	10
TAM110	54.7	a	4	46.5	a	2	50.7	a	2
TAM111	53.7	a	5	48.4	a	1	51.4	a	1
TAM112	49.7	a	8	44.5	a	3	47.4	a	6
TX86A5606	57.6	a	1	42.1	a	7	49.4	a	3
TX86A8072	49.1	a	10	43.6	a	4	46.6	a	8
TX88A6880	56.0	a	2	40.9	a	8	48.1	a	4
TX99A0153-1	49.2	a	9	43.4	a	5	46.6	a	9
Mean	52.8			43.1			47.9		

Despite clear contrasts in yield, TAM105 and TAM111 were both ranked among the highest in CTD under rainfed and irrigated conditions (Table 5.4). TAM112, which was one of the higher yielding cultivars under rainfed conditions, had one of the lowest CTDs under the same conditions. TAM105 and TAM112 are notable exceptions from the theory that higher CTD predicts better drought tolerance under rainfed conditions. Further, it suggests that cultivars may respond differently to water stress in regards to transpiration.

The yield rankings were compared against the CT and CTD rankings for each method (Tables 5.9 and 5.10, respectively). For all methods, the rank-shifts between yield and both CT and CTD were higher under rainfed conditions than under irrigated conditions. This was likely due to higher variance in stressed environments as was found by Gonzalez-Dugo et al. (2006). Indeed, under rainfed conditions, the average standard deviation of canopy temperature within a single plot measured using the TCAM were 3.40 and 3.68 for the narrow- and wide-angle lens, respectively, whereas the average standard deviation of canopy temperature within an irrigated plot were 1.39 and 1.06, respectively. The IRT had a lower average rank-shift with yield in both CT and CTD than the TCAM in both years under rainfed conditions. The IRT also had the highest correlation between yield and CT (Table 5.11), however, the IRT and TCAM-N had almost identical correlations between yield and CTD (Table 5.7). The TCAM methods both had lower average rank-shifts between both CT and CTD and yield than the IRT under irrigated conditions and yield was only significantly but weakly correlated to CT using the TCAM-W and to CTD using the TCAM-N ($r = 0.416$ and 0.236, respectively).

Table 5.9. Ranks and yield rank-shifts of canopy temperature at anthesis measured by infrared thermometer (IRT), thermal camera with narrow-angle lens (TCAM-N) and thermal camera with wide-angle lens (TCAM-W) of winter wheat cultivars grown under rainfed and irrigated regimes in Bushland, TX in 2009 and 2011.

	2009					2011						
	Yield	IRT		TCAM-N		Yield	IRT		TCAM-N		TCAM-W	
Cultivar	rank	rank	yield rank-shift	rank	yield rank-shift	rank	rank	yield rank-shift	rank	yield rank-shift	rank	yield rank-shift
Rainfed												
Dumas	5	3	2	7	2	9	4	1	6	1	5	0
Jagalene	4	7	3	6	2	6	5	1	2	2	10	6
TAM105	8	4	4	1	7	10	10	2	7	1	3	5
TAM110	1	6	5	3	2	1	8	7	9	8	2	1
TAM111	6	2	4	2	4	3	2	4	4	2	1	5
TAM112	3	8	5	10	7	4	6	3	10	7	7	4
TX86A5606	9	10	1	4	5	7	7	2	8	1	9	0
TX86A8072	10	9	1	8	2	2	3	7	1	9	4	6
TX88A6880	7	5	2	5	2	5	9	2	3	4	8	1
TX99A0153-1	2	1	1	9	7	8	1	1	5	3	6	4
Mean			2.8		4.0			3.0		3.8		3.2
Irrigated												
Dumas	7	5	2	2	5	3	10	3	7	0	7	0
Jagalene	3	3	0	8	5	6	1	2	2	1	3	0
TAM105	8	7	1	4	4	1	3	5	3	5	10	2
TAM110	6	4	2	6	0	7	2	4	4	2	6	0
TAM111	1	2	1	1	0	4	4	3	5	4	9	8
TAM112	4	6	2	3	1	9	9	5	9	5	1	3
TX86A5606	9	1	8	10	1	5	6	3	10	1	8	1
TX86A8072	10	9	1	9	1	10	8	2	6	4	4	6
TX88A6880	5	10	5	5	0	8	7	2	8	3	5	0
TX99A0153-1	2	8	6	7	5	2	5	3	1	1	2	0
Mean			2.8		2.2			3.2		2.6		2.0

Table 5.10. Ranks and yield rank-shifts of canopy temperature depression at anthesis measured by infrared thermometer (IRT), thermal camera with narrow-angle lens (TCAM-N) and thermal camera with wide-angle lens (TCAM-W) of winter wheat cultivars grown under rainfed and irrigated regimes in Bushland, TX in 2009 and 2011.

	2009					2011						
	Yield	IRT		TCAM-N		Yield	IRT		TCAM-N		TCAM-W	
Cultivar	rank	rank	yield rank-shift	rank	yield rank-shift	rank	rank	yield rank-shift	rank	yield rank-shift	rank	yield rank-shift
Rainfed												
Dumas	5	3	2	7	2	9	4	1	6	1	5	0
Jagalene	4	7	3	6	2	6	5	1	2	2	10	6
TAM105	8	4	4	1	7	10	10	2	7	1	3	5
TAM110	1	6	5	3	2	1	8	7	9	8	2	1
TAM111	6	2	4	2	4	3	2	4	4	2	1	5
TAM112	3	8	5	10	7	4	6	3	10	7	7	4
TX86A5606	9	10	1	4	5	7	7	2	8	1	9	0
TX86A8072	10	9	1	9	1	2	3	7	1	9	4	6
TX88A6880	7	5	2	5	2	5	9	2	3	4	8	1
TX99A0153-1	2	1	1	8	6	8	1	1	5	3	6	4
Mean			2.8		3.8			3.0		3.8		3.2
Irrigated												
Dumas	7	5	2	2	5	3	10	3	7	0	7	0
Jagalene	3	3	0	7	4	6	1	2	2	1	3	0
TAM105	8	7	1	4	4	1	3	5	4	4	10	2
TAM110	6	4	2	6	0	7	2	4	5	1	6	0
TAM111	1	2	1	1	0	4	4	3	3	2	9	8
TAM112	4	6	2	3	1	9	9	5	9	5	1	3
TX86A5606	9	1	8	10	1	5	6	3	10	1	8	1
TX86A8072	10	9	1	9	1	10	8	2	6	4	4	6
TX88A6880	5	10	5	5	0	8	7	2	8	3	5	0
TX99A0153-1	2	8	6	8	6	2	5	3	1	1	2	0
Mean			2.8		2.2			3.2		2.2		2.0

Table 5.11. Correlations between yield and canopy temperature at anthesis measured by infrared thermometer (IRT) and thermal camera with narrow-angle lens (TCAM-N) in 2009 and 2011, and thermal camera with wide-angle lens (TCAM-W) in 2011 of winter wheat grown under rainfed and irrigated regimes in Bushland, TX.

	Method		
Correlation with yield	IRT	TCAM-N	TCAM-W*
Rainfed			
Pearson correlation	-0.683	-0.606	-0.182
P-value	<0.0001	<0.0001	0.2599
No. observations	100	100	40
Irrigated			
Pearson correlation	-0.092	-0.147	0.416
P-value	0.5299	0.1691	0.0247
	49	89	29
Combined			
Pearson correlation	-0.908	-0.810	-0.968
P-value	<0.0001	<0.0001	<0.0001
No. observations	149	189	69

* TCAM-W had only one year of data (2011) with 4 replications on the rainfed field and 3 replications on the irrigated field

Overall, it appears that the IRT was better at ranking yields under rainfed conditions whereas the TCAM methods were better at ranking yields under irrigated conditions. However, this assumes that CTD is positively related to yield, which does not appear to be the case for all cultivars (TAM112, for example).

There was a significant positive relationship between percent ground cover and yield under rainfed conditions ($r = 0.528$ and 0.317 using the TCAM-N and TCAM-W, respectively). However, there were no significant differences in percent ground cover between cultivars. Therefore, it is unlikely that any differences in cultivar establishment, emergence, or planting density had any confounding effects on yield. Nonetheless,

TAM111 had the highest percent ground cover across years whereas TAM105 had the lowest (Table 5.8). This corresponded to their respective yields under rainfed conditions (Table 5.5).

5.4 Conclusions

This study suggests that under field conditions such as our, the adjusted means of canopy temperature using vapor pressure deficit and wind speed as covariates in the model can substitute for measurements of canopy temperature depression for the purpose of ranking cultivars. Of the cultivars assessed, TAM110 had the highest yield under rainfed conditions whereas TAM111 had the highest yields under irrigated conditions. TAM111 was both drought tolerant and responsive to irrigation, TAM110 was drought tolerant but less responsive to irrigation, and TAM105 was drought susceptible and responsive to irrigation. Although TAM111 and TAM112 (closely related) were both high yielding under rainfed conditions, they ranked among the highest and lowest in CTD, respectively. Therefore, CTD was not always a reliable indicator of yield for every variety under rainfed conditions. This should be considered when making selections based on CTD. In a combined analysis across years, TX86A5606 ranked the warmest and was significantly warmer than TX99A0153-1 under rainfed conditions and significantly warmer than TAM111 under irrigated conditions. TX86A5606 also ranked among the lowest in yield in both regimes. Under rainfed conditions, the canopy temperature measured with the IRT had the highest correlation and the lowest rank-shift with yield. Under irrigated conditions, the canopy temperature measured using the TCAM-N and IRT had similar correlations with yield but both TCAM methods had a

lower rank-shift with yield than the IRT. Under rainfed conditions, the TCAM was able to measure percent ground cover that was significantly correlated with yield. However, there were no significant differences in percent ground cover between cultivars.

Shading can be an important factor in measuring canopy temperature. In the morning when the sun is low, the TCAM positioned overhead may capture a greater amount of shaded plants than the IRT. However, the angle and direction of the IRT with respect to the sun can have a substantial influence. Conversely, when the sun is directly overhead, the TCAM overhead captures almost no shading whereas the IRT positioned at a 45-degree angle from eye-level captures substantially more shaded plant area.

This study reveals both the potential as well as the limitations of using thermal imaging for high-throughput phenotyping of canopy temperature in winter wheat. In this study, we developed methodologies to capture thermal images of field plots and software to analyze thermal images rapidly. Future research should employ this technology to assess cultivars in more diverse environments with a particular emphasis on the genotype by environment interaction as it pertains to adaptability.

6. CONCLUSION

In cowpea, trifoliate necrosis was found to be a more reliable predictor of death than wilting or unifoliate necrosis. Stem diameter was highly correlated with resistance to lodging, and unifoliate and trifoliate necrosis suggesting that carbohydrates stored in the stem may help mitigate water stress. A unifoliate stay-green trait was discovered which segregates as a single recessive gene. However, it did not co-segregate with resistance to trifoliate necrosis which previous research has shown to be a single dominant gene. Therefore, it is likely "non-functional" and does not appear to confer drought-tolerance.

Leaf water content in cowpea trifoliates was largely maintained during water stress and had no correspondence to the level or type of drought tolerance. However, water stress did reduce net photosynthesis, stomatal conductance and transpiration similarly for all cowpea cultivars. At the same time, the intercellular CO_2 concentration increased suggesting that reduced photosynthesis was not due to the stomata limiting CO_2 availability or photorespiration. During the early stages of water stress, photosynthesis rapidly declined and the unifoliates of susceptible cultivars began to senesce while the younger trifoliates and the stems and petioles continued to increase in dry weight. This suggests that excess photosynthate was exported from the younger leaves and stored in the stems and petioles. Elevated intercellular CO_2 concentrations and the possible export of excess photosynthate from the leaves suggest an end-product inhibition of photosynthesis due to the accumulation of carbohydrates. Early unifoliate

senescence exhibited by certain cultivars did not appear to be due to declining leaf water content nor did it appear to improve overall plant water status. Therefore, it may be a general stress response and have little effect in mitigating drought tolerance.

The Software developed to analyze thermal images has proved invaluable for processing hundreds of thermal images in multiple studies. The two-means filtering algorithm was found to be highly robust and adaptable to many environments. However, it depends on a sufficient amount of visible soil in each image. In cases with a low amount of visible soil, no filtering is necessary. The peak-detection algorithm with masking also proved useful for batch processing of images with a stationary thermal imaging device and little leaf movement. Nonetheless, additional research could greatly improve this algorithm's performance by determining the optimal bin size and the optimal parameters for the filter and decay functions. Both filtering algorithms rely on thermal images having good contrast between the soil and canopy temperatures and a low variance of each.

In winter wheat, the adjusted means of canopy temperature with vapor pressure deficit and wind speed as covariates in the model can substitute for measurements of canopy temperature depression and eliminate the need of reference plots for the purpose of ranking cultivars. Of the cultivars assessed, TAM111 was both drought tolerant and responsive to irrigation, TAM110 was drought tolerant but less responsive to irrigation, and TAM105 was drought susceptible and responsive to irrigation. Although TAM111 and TAM112 (closely related) were both high yielding under rainfed conditions, they ranked among the highest and lowest in CTD, respectively. Therefore, CTD did not

always predict yield under rainfed conditions likely due to multiple contrasting mechanisms of drought tolerance. Therefore, no single method of phenotyping for drought tolerance can be broadly applied across all genotypes of a given species.

REFERENCES

Amani, I., R.A. Fischer, and M.P. Reynolds. 1996. Canopy temperature depression association with yield of irrigated spring wheat cultivars in a hot climate. J. Agron. and Crop Sci. 176:119-129.

Anyia, A.O., and H. Herzog. 2004. Water-use efficiency, leaf area and leaf gas exchange of cowpeas under mid-season drought. Eur. J. Agron. 20:327-339.

Auge, R.M., A.J.W. Stodola, M.S. Brown, and G.J. Bethlenfalvay. 1992. Stomatal response of mycorrhizal cowpea and soybean to short-term osmotic stress. New Phytol. 120:117-125.

Balota, M., W.A. Payne, S.R. Evett, and M.D. Lazar. 2007. Canopy temperature depression sampling to assess grain yield and genotypic differentiation in winter wheat. Crop Sci. 47:1518-1529.

Balota, M., W.A. Payne, S.R. Evett, and T.R. Peters. 2008. Morphological and physiological traits associated with canopy temperature depression in three closely related wheat lines. Crop Sci. 48:1897-1910.

Bates, L.M., and A.E. Hall. 1981. Stomatal closure with soil water depletion not associated with changes in bulk leaf water status. Oecologia 50:62-65.

Bates, L.M., and A.E. Hall. 1982. Diurnal and seasonal responses of stomatal conductance for cowpea plants subjected to different levels of environmental drought. Oecologia 54:304-308.

Blum, A. 1989. The temperature response of gas exchange in sorghum leaves and the effect of heterosis. J. Exp. Bot. 40:453.

Blum, A., J. Mayer, and G. Gozlan. 1982. Infrared thermal sensing of plant canopies as a screening technique for dehydration avoidance in wheat. Field Crops Res. 5:137-146.

Blum, A., L. Shpiler, G. Golan, and J. Mayer. 1989. Yield stability and canopy temperature of wheat genotypes under drought-stress. Field Crops Res. 22:289-296.

Contour-Ansel, D., M.L. Torres-Franklin, M.H. Cruz de Carvalho, A. d'Arcy-Lameta, and Y. Zuily-Fodil. 2006. Glutathione reductase in leaves of cowpea: Cloning of two cDNAs, expression and enzymatic activity under progressive drought stress, desiccation and abscisic acid treatment. Ann. Bot. 98:1279-1287.

Cornic, G., and J.M. Briantais. 1991. Partitioning of photosynthetic electron flow between CO_2 and O_2 reduction in a C3 leaf (*Phaseolus vulgaris* L.) at different CO_2 concentrations and during drought stress. Planta 183:178-184.

Costa, J.H., Y. Jolivet, M.P. Hasenfratz-Sauder, E.G. Orellano, M. da Guia Silva Lima, P. Dizengremel, and D. Fernandes de Melo. 2007. Alternative oxidase regulation in roots of *Vigna unguiculata* cultivars differing in drought/salt tolerance. J. of Plant Physiol. 164:718-727.

Crafts-Brandner, S.J., F.E. Below, J.E. Harper, and R.H. Hageman. 1984. Effects of pod removal on metabolism and senescence of nodulating and nonnodulating soybean isolines: I. Metabolic constituents. Plant Physiol. 75:311-317.

Cruz de Carvalho, M.H., D. Laffray, and P. Louguet. 1998. Comparison of the physiological responses of *Phaseolus vulgaris* and *Vigna unguiculata* cultivars when submitted to drought conditions. Environ. and Exp. Bot. 40:197-207.

Ehrler, W.L. 1973. Cotton leaf temperatures as related to soil water depletion and meteorological factors. Agron. J. 65:404-409.

Epron, D., E. Dreyer, and N. Breda. 1992. Photosynthesis of oak trees [*Quercus petraea* (Matt.) Liebl.] during drought under field conditions: diurnal course of net CO_2 assimilation and photochemical efficiency of photosystem II. Plant Cell Environ. 15:809-820.

Fang, J., C.C.T. Chao, P.A. Roberts, and J.D. Ehlers. 2007. Genetic diversity of cowpea [*Vigna unguiculata* (L.) Walp.] in four West African and USA breeding programs as determined by AFLP analysis. Genetic Resources and Crop Evolution 54:1197-1209.

Ferguson, H.E., and R.F. Aase. 1973. Canopy temperatures of barley as influenced by morphological characteristics. Agron. J. 65:425-428.

Fischer, R.A., D. Rees, K.D. Sayre, Z.M. Lu, A.G. Condon, and A.L. Saavedra. 1998. Wheat yield progress associated with higher stomatal conductance and photosynthetic rate, and cooler canopies. Crop Sci. 38:1467-1475.

Francois, C., C. Ottlé, and L. Prévot. 1997. Analytical parameterization of canopy directional emissivity and directional radiance in the thermal infrared. Application on the retrieval of soil and foliage temperatures using two directional measurements. Int. J. Remote Sens. 18:2587-2621.

Giuliani, R., and J.A. Flore. 1999. Potential use of infra-red thermometry for the detection of water stress in apple trees. Acta Hort. (ISHS) 537:383-392.

Global Development Program. 2011. Agricultural development strategic overview. Bill & Melinda Gates Foundation. http://www.gatesfoundation.org/agricultural development/Documents/agricultural-development-strategy-overview.pdf (accessed 11 Nov. 2011).

Graham, P.H., and C.P. Vance. 2003. Legumes: importance and constraints to greater use. Plant Physiol. 131:872-877.

Gonzalez-Dugo, M.P., M.S. Moran, L. Mateos, and R. Bryant. 2006. Canopy temperature variability as an indicator of crop water stress severity. Irrig. Sci. 24:233-240.

Gwathmey, C.O., A.E. Hall, and M.A. Madore. 1992. Adaptive attributes of cowpea genotypes with delayed monocarpic leaf senescence. Crop Sci. 32:765-772.

Hall, A.E., and E. Schulze. 1980. Drought effects on transpiration and leaf water status of cowpea in controlled environments. Funct. Plant Biol. 7:141-147.

Hamidou, F., G. Zombre, and S. Braconnier. 2007. Physiological and biochemical responses of cowpea genotypes to water stress under glasshouse and field conditions. J. Agron. Crop Sci. 193:229-237.

Hinckley, T.M., and D.N. Bruckerhoff. 2011. The effects of drought on water relations and stem shrinkage of *Quercus alba*. Can. J. Bot. 53:62-72.

Huber, S.C., H.H. Rogers, and F.L. Mowry. 1984. Effects of water stress on photosynthesis and carbon partitioning in soybean (*Glycine max* [L.] Merr.) plants grown in the field at different CO_2 levels. Plant Physiol. 76:244-249.

Idso, S.B. 1982. Non-water-stressed baselines: A key to measuring and interpreting plant water stress. Agric. Forest Meteorol. 27:59-70.

Idso, S.B., B.A. Kimball, and K.L. Clawson. 1984. Quantifying effects of atmospheric CO_2 enrichment on stomatal conductance and evapotranspiration of water hyacinth via infrared thermometry. Agric. For. Meteorol. 33:15-22.

Jackson, R.D., S.B. Idso, R.J. Reginato, and W.L. Ehrler. 1977. Crop temperature reveals stress. Crops Soils 29:10-13.

Jackson, R.D., S.B. Idso, R.J. Reginato, and P.J. Pinter Jr. 1981. Canopy temperature as a crop water stress indicator. Water Resour. Res. 17:1133-1138.

Jones, H.G. 1999. Use of thermography for quantitative studies of spatial and temporal variation of stomatal conductance over leaf surfaces. Plant Cell Environ. 22:1043-1055.

Jones, H.G. 2004. Irrigation scheduling: advantages and pitfalls of plant-based methods. J. Exp. Bot. 55:2427-2436.

Jones, H.G., D. Aikman, and T.A. McBurney. 1996. Improvements to infra-red thermometry for irrigation scheduling in humid climates. Acta Hort. (ISHS) 449:259-266.

Jones, H.G., and I. Leinonen. 2003. Thermal imaging for the study of plant water relations. J. Agric. Meteorol. 59:205-217.

Jones, H.G., M. Stoll, T. Santos, C. Sousa, M.M. Chaves, and O.M. Grant. 2002. Use of infrared thermography for monitoring stomatal closure in the field: application to grapevine. J. Exp. Bot. 53:2249-2260.

Kimes, D.S., S.B. Idso, P.J. Pinter Jr, R.J. Reginato, and R.D. Jackson. 1980. View angle effects in the radiometric measurement of plant canopy temperatures. Remote Sens. Environ. 10:273-284.

Kundzewicz, Z.W., L.J. Mata, N.W. Arnell, P. Döll, P. Kabat, B. Jiménez, K.A. Miller, T. Oki, Z. Sen, and I.A. Shiklomanov. 2008. Climate Change 2007: Impacts, Adaptation and Vulnerability. Contribution of working group II to the fourth assessment report of the intergovernmental panel on climate change. Cambridge University Press, Cambridge, UK. p. 173-210.

Küppers, B.I.L., M. Küppers, and E.D. Schulze. 1988. Soil drying and its effect on leaf conductance and CO_2 assimilation of *Vigna unguiculata* (L.) Walp. Oecologia 75:99-104.

Leinonen, I., and H.G. Jones. 2004. Combining thermal and visible imagery for estimating canopy temperature and identifying plant stress. J. Exp. Bot. 55:1423-1431.

Mai-Kodomi, Y., B.B. Singh, O. Myers, J.H.J. Yopp, P.J. Gibson, and T. Terao. 1999a. Two mechanisms of drought tolerance in cowpea. Indian J. Genet. Plant Breed. 59:309-316.

Mai-Kodomi, Y., B.B. Singh, T. Terao, O. Myers, J.H.J. Yopp, and P.J. Gibson. 1999b. Inheritance of drought tolerance in cowpea. Indian J. Genet. Plant Breed. 59:317-323.

Manivannan, P., C. Abdul Jaleel, A. Kishorekumar, B. Sankar, R. Somasundaram, R. Sridharan, and R. Panneerselvam. 2007. Changes in antioxidant metabolism of *Vigna unguiculata* (L.) Walp. by propiconazole under water deficit stress. Colloids and Surfaces B: Biointerfaces 57:69-74.

Merlot, S., A.C. Mustilli, B. Genty, H. North, V. Lefebvre, B. Sotta, A. Vavasseur, and J. Giraudat. 2002. Use of infrared thermal imaging to isolate Arabidopsis mutants defective in stomatal regulation. Plant J. 30:601–609.

Morgan, J.M. 1984. Osmoregulation and water stress in higher plants. Annual Review of Plant Physiol. 35:299-319.

Mustilli, A. C., Merlot, S., Vavasseur, A., Fenzi, F. and Giraudat, J. (2002). Arabidopsis OST1 protein kinase mediates the regulation of stomatal aperture by abscisic acid and acts upstream of reactive oxygen species production. Plant Cell. 14:3089-3099.

Noctor, G., and C.H. Foyer. 1998. Ascorbate and glutathione: Keeping active oxygen under control. Annu. Rev. Plant Physiol. Plant Mol. Biol 49:249-279.

Ohashi, Y., N. Nakayama, H. Saneoka, and K. Fujita. 2006. Effects of drought stress on photosynthetic gas exchange, chlorophyll fluorescence and stem diameter of soybean plants. Biologia Plantarum 50:138-141.

Pinter, P.J. 1990. Canopy temperature as an indicator of differential water use and yield performance among wheat cultivars. Agric. Water Manage. 18:35-48.

Rashid, A., J.C. Stark, A. Tanveer, and T. Mustafa. 1999. Use of canopy temperature measurements as a screening tool for drought tolerance in spring wheat. J. Agron. Crop Sci. 182:231-238.

Reynolds, M.P., M. Balota, M.I.B. Delgado, I. Amani, and R.A. Fischer. 1994. Physiological and morphological traits associated with spring wheat yield under hot, irrigated conditions. Funct. Plant Biol. 21:717-730.

Royo, C., D. Villegas, L.F.G. del Moral, S. Elhani, N. Aparicio, Y. Rharrabti, and J.L. Araus. 2002. Comparative performance of carbon isotope discrimination and canopy temperature depression as predictors of genotype differences in durum wheat yield in Spain. Aust. J. Agric. Res. 53:561-570.

Schakel, K.A., and A.E. Hall. 1979. Reversible leaflet movements in relation to drought adaptation of cowpeas, *Vigna unguiculata* (L.) Walp. Funct. Plant Biol. 6:265-276.

Simonneau, T., R. Habib, J.P. Goutouly, and J.G. Huguet. 1993. Diurnal changes in stem diameter depend upon variations in water content: direct evidence in peach trees. J. Exp. Bot. 44:615-621.

Singh, B.B., Y. Mai-Kodomi, and T. Terao. 1999. A simple screening method for drought tolerance in cowpea. Indian J. Genet. Plant Breed. 59:211-220.

Smith, W.K. 1978. Temperatures of desert plants: another perspective on the adaptability of leaf size. Science 201:614-616.

Sojka, R.E., E.J. Sadler, C.R. Camp, and F.B. Arnold. 1990. A comparison of pressure chamber, leaf-press, and canopy temperature for four species under humid conditions. Environ. Exp. Bot. 30:75-83.

Souza, R.P., E.C. Machado, J.A.B. Silva, A. Lagoa, and J.A.G. Silveira. 2004. Photosynthetic gas exchange, chlorophyll fluorescence and some associated metabolic changes in cowpea (*Vigna unguiculata*) during water stress and recovery. Environ. Exp. Bot. 51:45-56.

Teare, I.D., and E.T. Kanemasu. 1972. Stomatal-diffusion resistance and water potential of soybean and sorghum leaves. New Phytol. 71:805-810.

Winter, S.R., and J.T. Porter. 1988. Evaluation of screening techniques for breeding drought-resistant winter wheat. Crop Sci. 28:512-516.

APPENDIX A

SUPPLEMENTAL DATA FOR GENETICS AND HERITABILITY OF DROUGHT TOLERANCE IN COWPEA STUDY

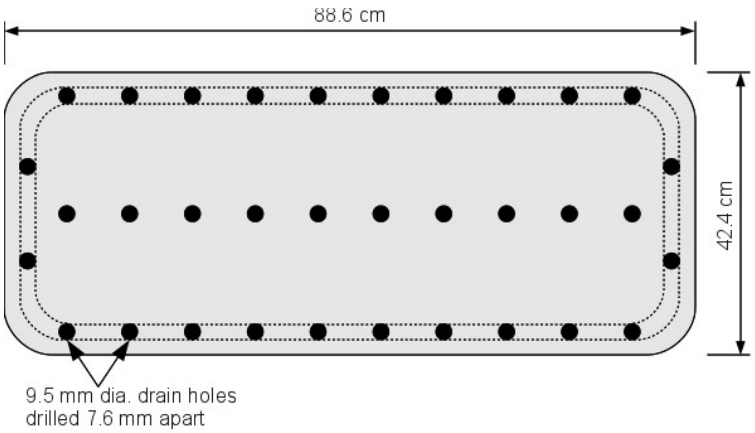

Figure A-1. Layout of drainage holes for drought screening boxes.

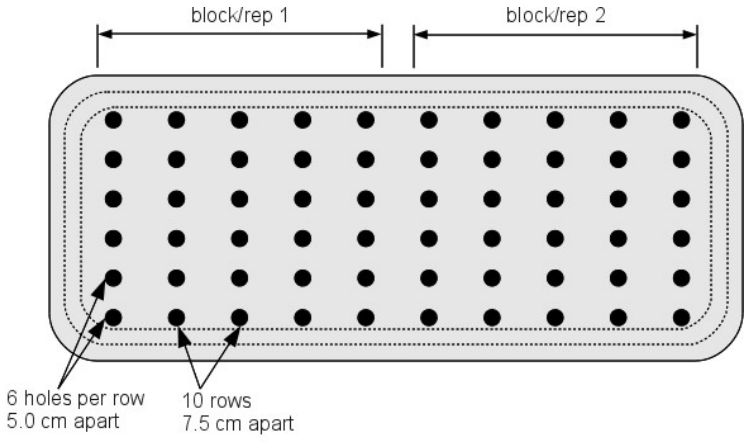

Figure A-2. Layout of planting holes for drought screening boxes.

Figure A-3. Image of box screening experiment for cowpea seedlings grown in a growth room under terminal water stress conditions.

Figure A-4. Drought box screening of cowpea seedlings after 45 days of withholding water shows clear differences between rows of different cultivars.

APPENDIX B

SUPPLEMENTAL DATA FOR PHYSIOLOGY OF DROUGHT TOLERANCE IN COWPEA STUDY

Table B-1. Average leaf dry weight per plant over time of three replications of cowpea cultivars grown in a greenhouse under terminal water stress.

	Days of Stress									
Cultivar	3		7		10		15		18	
					G					
CB27	0.81	a	0.76	a	0.80	a	0.63	a	0.77	a
CB46	0.76	a	0.87	a	0.79	a	0.72	a	0.73	a
IT97K-556-4	0.67	a	0.82	a	0.68	a	0.89	a	0.77	a
IT99K-241-2	0.64	a	0.75	a	0.70	a	0.74	a	0.71	a
TVu-7778	0.65	a	0.76	a	0.75	a	0.58	a	0.62	a
TX2028-1-3-1	0.62	a	0.82	a	0.82	a	0.76	a	0.77	a

Table B-2. Average stem and petiole dry weight per plant over time of three replications of cowpea cultivars grown in a greenhouse under terminal water stress.

	Days of Stress									
Cultivar	3		7		10		15		18	
					g					
CB27	0.39	a	0.45	ab	0.40	a	0.29	b	0.39	a
CB46	0.40	a	0.51	ab	0.42	a	0.42	ab	0.44	a
IT97K-556-4	0.43	a	0.59	a	0.44	a	0.52	a	0.53	a
IT99K-241-2	0.45	a	0.47	ab	0.45	a	0.45	ab	0.55	a
TVu-7778	0.33	a	0.34	b	0.35	a	0.33	ab	0.42	a
TX2028-1-3-1	0.40	a	0.45	ab	0.42	a	0.43	ab	0.49	a

Table B-3. Average total dry matter over time of three replications of cowpea cultivars grown in a greenhouse under terminal water stress.

	Days of Stress									
Cultivar	3		7		10		15		18	
					g					
CB27	1.20	a	1.21	a	1.20	a	0.92	a	1.17	a
CB46	1.15	a	1.39	a	1.21	a	1.13	a	1.17	a
IT97K-556-4	1.10	a	1.41	a	1.12	a	1.41	a	1.30	a
IT99K-241-2	1.09	a	1.23	a	1.16	a	1.18	a	1.26	a
TVu-7778	0.97	a	1.10	a	1.10	a	0.91	a	1.04	a
TX2028-1-3-1	1.01	a	1.26	a	1.24	a	1.19	a	1.26	a

Table B-4. Average soil moisture content per pot over time of three replications of cowpea cultivars grown in a greenhouse under terminal water stress.

	Days of Stress									
Cultivar	3		7		10		15		18	
					%					
CB27	44.7	a	33.4	a	23.2	a	21.8	a	10.8	a
CB46	50.5	a	30.8	a	22.2	a	17.1	a	11.5	a
IT97K-556-4	49.8	a	38.0	a	32.9	a	17.8	a	11.6	a
IT99K-241-2	51.0	a	39.3	a	31.4	a	17.6	a	14.1	a
TVu-7778	50.1	a	38.1	a	23.9	a	16.5	a	12.1	a
TX2028-1-3-1	49.0	a	32.2	a	27.9	a	13.6	a	11.7	a

Table B-5. Average single leaf dry weights over time of three replications of cowpea cultivars grown in a greenhouse under terminal water stress.

	Days of Stress									
Cultivar	3		7		10		15		18	
					g					
Unifoliate										
CB27	0.17	a	0.08	a	0.13	a	0.10	a	0.13	ab
CB46	0.14	ab	0.10	a	0.06	a	0.09	a	0.09	cd
IT97K-556-4	0.13	ab	0.10	a	0.09	a	0.12	a	0.11	abc
IT99K-241-2	0.10	ab	0.11	a	0.09	a	0.10	a	0.10	bc
TVu-7778	0.09	b	0.11	a	0.08	a	0.08	a	0.06	d
TX2028-1-3-1	0.12	ab	0.13	a	0.13	a	0.13	a	0.14	a
1st trifoliate										
CB27	0.09	a	0.10	a	0.09	a	0.08	a	0.09	a
CB46	0.09	a	0.12	a	0.10	a	0.09	a	0.11	a
IT97K-556-4	0.08	a	0.07	a	0.07	a	0.12	a	0.09	a
IT99K-241-2	0.09	a	0.10	a	0.11	a	0.10	a	0.10	a
TVu-7778	0.09	a	0.12	a	0.11	a	0.08	a	0.09	a
TX2028-1-3-1	0.07	a	0.12	a	0.09	a	0.11	a	0.09	a
2nd trifoliate										
CB27	0.06	a	0.08	a	0.09	a	0.06	a	0.09	a
CB46	0.07	a	0.09	a	0.11	a	0.09	a	0.09	a
IT97K-556-4	0.06	a	0.11	a	0.07	a	0.10	a	0.09	a
IT99K-241-2	0.06	a	0.13	a	0.07	a	0.09	a	0.08	a
TVu-7778	0.06	a	0.10	a	0.07	a	0.07	a	0.06	a
TX2028-1-3-1	0.06	a	0.10	a	0.09	a	0.07	a	0.07	a

Table B-6. Average carbon assimilation rates over time of three replications of the youngest fully-expanded trifoliate of cowpea cultivars grown in a greenhouse under terminal water stress.

	Days of Stress									
Cultivar	3		7		10		15		18	
	μmol m^{-2} s^{-1}									
CB27	8.52	a	6.90	a	0.83	a	0.37	a	-0.09	a
CB46	6.93	a	2.66	a	0.39	a	0.40	a	-0.17	a
IT97K-556-4	10.07	a	2.99	a	4.26	a	0.63	a	-0.15	a
IT99K-241-2	7.88	a	5.57	a	2.05	a	0.56	a	0.37	a
TVu-7778	8.97	a	6.05	a	0.67	a	0.13	a	-0.08	a
TX2028-1-3-1	9.17	a	5.06	a	2.87	a	0.19	a	-0.14	a

Table B-7. Average stomatal conductance over time of three replications of the youngest fully-expanded trifoliate of cowpea cultivars grown in a greenhouse under terminal water stress.

	Days of Stress									
Cultivar	3		7		10		15		18	
	mmol m^{-2} s^{-1}									
CB27	0.25	a	0.23	ab	0.14	a	0.03	a	0.00	a
CB46	0.22	a	0.15	b	0.10	a	0.03	a	0.00	a
IT97K-556-4	0.26	a	0.20	ab	0.23	a	0.03	a	0.00	a
IT99K-241-2	0.26	a	0.29	a	0.17	a	0.04	a	0.01	a
TVu-7778	0.23	a	0.28	a	0.16	a	0.03	a	0.00	a
TX2028-1-3-1	0.23	a	0.17	b	0.17	a	0.02	a	0.00	a

Table B-8. Average intercellular CO_2 concentration over time of three replications of the youngest fully-expanded trifoliate of cowpea cultivars grown in a greenhouse under terminal water stress.

	Days of Stress									
Cultivar	3		7		10		15		18	
	μL L^{-1}									
CB27	231.6	a	309.0	a	373.9	a	350.2	a	439.1	a
CB46	242.6	a	351.4	a	372.7	a	352.3	a	553.2	a
IT97K-556-4	256.6	a	359.7	a	335.9	a	343.5	a	468.7	a
IT99K-241-2	268.2	a	337.0	a	352.8	a	352.9	a	398.9	a
TVu-7778	241.0	a	338.2	a	367.7	a	377.8	a	440.8	a
TX2028-1-3-1	239.5	a	311.9	a	351.5	a	363.2	a	465.0	a

Table B-9. Average transpiration rates over time of three replications of the youngest fully-expanded trifoliate of cowpea cultivars grown in a greenhouse under terminal water stress.

	Days of Stress									
Cultivar	3		7		10		15		18	
	mmol m-2 s-1									
CB27	10.70	a	6.30	Ab	4.88	bc	1.30	a	0.07	a
CB46	8.52	a	5.02	B	4.63	c	1.20	a	0.05	a
IT97K-556-4	11.10	a	6.10	Ab	7.68	ab	1.32	a	0.09	a
IT99K-241-2	10.33	a	7.77	A	7.75	a	1.87	a	0.15	a
TVu-7778	7.07	a	7.65	A	8.30	a	1.25	a	0.07	a
TX2028-1-3-1	8.35	a	5.28	B	5.60	abc	1.35	a	0.08	a

Table B-10. Average instantaneous water use efficiency over time of three replications of the youngest fully-expanded trifoliate of cowpea cultivars grown in a greenhouse under terminal water stress.

	Days of Stress									
Cultivar	3		7		10		15		18	
	mmol m^{-2} s^{-1}									
CB27	10.70	a	6.30	ab	4.88	bc	1.30	a	0.07	a
CB46	8.52	a	5.02	b	4.63	c	1.20	a	0.05	a
IT97K-556-4	11.10	a	6.10	ab	7.68	ab	1.32	a	0.09	a
IT99K-241-2	10.33	a	7.77	a	7.75	a	1.87	a	0.15	a
TVu-7778	7.07	a	7.65	a	8.30	a	1.25	a	0.07	a
TX2028-1-3-1	8.35	a	5.28	b	5.60	abc	1.35	a	0.08	a

Table B-11. Average leaf water content over time of cowpea cultivars grown in a greenhouse under terminal water stress.

	Days of Stress									
Cultivar	3		7		10		15		18	
					%					
Unifoliate										
CB27	87.9	b	91.2	a	88.3	a	86.7	a	86.0	ab
CB46	89.0	ab	92.1	a	95.3	a	86.8	a	77.8	b
IT97K-556-4	89.9	a	92.7	a	91.4	a	86.8	a	85.6	ab
IT99K-241-2	89.0	ab	87.1	a	89.6	a	87.2	a	87.7	a
TVu-7778	89.4	a	84.7	a	84.4	a	86.4	a	86.0	ab
TX2028-1-3-1	89.0	ab	89.0	a	86.7	a	87.2	a	86.2	ab
1st trifoliate										
CB27	87.1	a	82.8	a	83.1	a	84.5	a	83.2	a
CB46	86.0	a	87.0	a	82.3	a	85.1	a	80.9	a
IT97K-556-4	86.1	a	89.6	a	87.1	a	84.6	a	83.7	a
IT99K-241-2	85.8	a	83.4	a	85.9	a	84.4	a	85.3	a
TVu-7778	87.2	a	79.8	a	82.0	a	84.6	a	83.4	a
TX2028-1-3-1	86.7	a	78.5	a	86.5	a	84.3	a	83.1	a
2nd trifoliate										
CB27	85.9	a	87.9	a	86.2	a	84.8	a	82.8	a
CB46	86.4	a	80.4	ab	80.1	a	84.4	a	80.4	a
IT97K-556-4	84.6	a	77.7	ab	77.7	a	83.0	a	83.1	a
IT99K-241-2	84.6	a	69.1	b	85.9	a	82.8	a	83.1	a
TVu-7778	85.5	a	78.4	ab	83.9	a	84.0	a	81.9	a
TX2028-1-3-1	85.9	a	80.7	ab	83.5	a	82.4	a	82.6	a

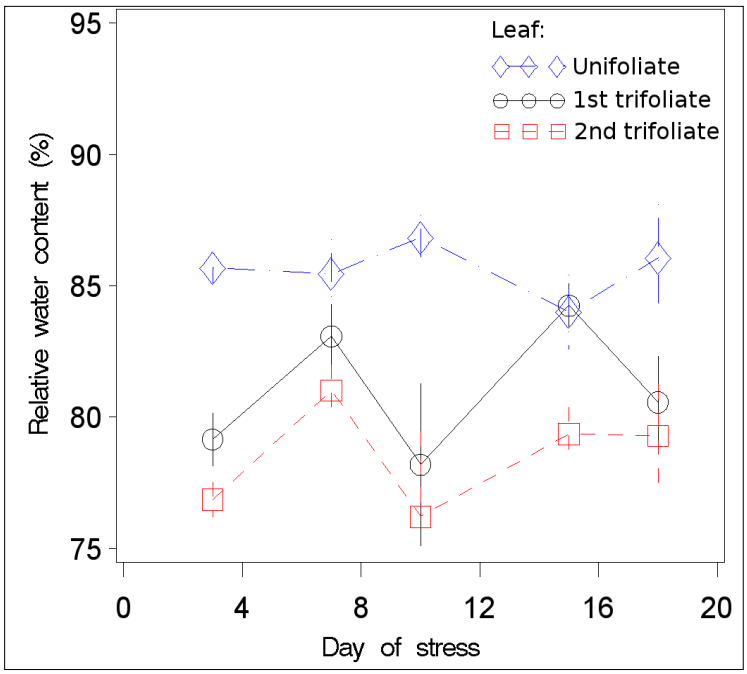

Figure B-1. Average relative water content over time of three replications of cowpea cultivars grown in a greenhouse under terminal water stress.

APPENDIX C

SUPPLEMENTAL INFORMATION FOR THERMAL IMAGE ANALYSIS SOFTWARE FOR BREEDERS AND PHYSIOLOGISTS

Pseudo-code

Box C-1. Pseudo-code for the two-means cluster filtering algorithm.

```
// k-means clustering where k=2
k1Center = minimum temperature of image
k2Center = maximum temperature of image
oldK1Center = 0
do
        oldK1Center = k1Center
        k1Sum = 0
        k1Cnt = 0
        k2Sum = 0
        k2Cnt = 0

        loop through each temperature reading in image (tempC)
                k1Dist = abs(tempC-k1Center)
                k2Dist = abs(tempC-k2Center)

                if (k1Dist < k2Dist)
                        k1Sum+=tempC;
                        k1Cnt++;
                else
                        k2Sum+=tempC;
                        k2Cnt++;
                end if

                //Calculate new centers
                k1Center = k1Sum / k1Cnt
                k2Center = k2Sum / k2Cnt
        end loop
```

Box C-1 (continued)

```
while abs(oldK1Center-k1Center) > 0.005
thresholdTemp = (k1Center + k2Center) / 2
```

Box C-2. Pseudo-code for the bi-modal peak-detection filter algorithm.

```
divide the temperature range of the image into 50 bins
place each temperature into the appropriate bin

loop through the count of each bin
        count = highPassFilter(count, 0.97)
        count = lowPassFilter(count, 0.60)
        count = movingAvgFilter(count, 4)

        meter = decayFunction(meter, 0.05)
        if count > meter
                // peak detected in the temperature range of the current bin, record it
                peakDetected = true
        else if peakDetected == true
                // count < decay function's meter, therefore peak is over
thresholdTemp = (peak1Temp + peak2Temp) / 2
```

Box C-3. Pseudo-code for the high-pass filter.

```
prevOutput = 0
prevInput = 0
function highPassFilter(newInput, alpha)
        newOutput = prevOutput + alpha * (newInput – prevInput)
        prevInput = newInput
        prevOutput = newOutput
        return newOutput
```

Box C-4. Pseudo-code for the low-pass filter.

```
prevOutput = 0
prevInput = 0
function lowPassFilter(newInput, alpha)
        newOutput = prevInput + alpha * (newInput – prevOutput)
        prevInput = newInput
        prevOutput = newOutput
        return newOutput
```

Box C-5. Pseudo-code for the decay-function.

```
function decayFunction(meter, epsilon)
        return (1-epsilon)*meter
```

Software design requirements

- The Software shall be portable with full functionality on Microsoft Windows XP, Microsoft Windows Vista, Ubuntu Linux, and Apple Mac OS 10 platforms.
- The Software shall read thermal images encoded in the FLIR Public Format
- The user shall have the ability to select target areas of thermal images for analysis, to assign identifiers to selected areas, save selections to a file and restore selections from a file
- The user shall have the ability to manually set filter temperature ranges in the Software
- The Software shall automatically filter out non-target areas from thermal images based on temperature thresholds

- The Software shall log pixel count, mean, min, max, and standard deviation for each user selected area to a comma-separated values (CSV) text file
- The Software shall run in batch mode to process a large number of images without user input between each image
- The Software shall be able to save selections to a CSV text file and restore them from a CSV text file
- Documentation shall be written to accompany the Software sufficient to allow others to learn to use the Software

APPENDIX D

COMPARISON OF ROOT TRAITS IN WINTER WHEAT USING RHIZOTRONS

Introduction

In the experiment described in Section 5, two closely related winter wheat cultivars, TAM111 and TAM112, were opposite in canopy temperature under rainfed conditions. TAM111 was one of the coolest cultivars whereas TAM112 was one of the hottest cultivars. Both cultivars are known as being highly drought-tolerant under field conditions. Therefore, it is hypothesized that TAM111, with a cooler canopy and higher transpiration rates, must have a root system capable of accessing soil moisture perhaps from deeper in the soil profile. Four rhizotrons were designed and constructed to compare the rate of root growth and root morphology of TAM111 and TAM112.

Materials and methods

The 2’ x 4’ rhizotrons were constructed out of 2” x 4” (nominally 1.5” x 3.5”) wooden members with a 5/8” plywood back (Figure D-2 and Figure D-3). A PVC liner was glued to the inside of each rhizotron to protect the wood from water damage. A 3/8” Plexiglas face was screwed to the front of each rhizotron through foam tape weather stripping to provide a water-tight seal. Three 5/8” drain holes were drilled into the bottom of each rhizotron and PVC drain tubes were glued into each hole.

Four rhizotrons was filled with Metro-mix® 700 planting media (Sun Gro Horticulture Canada CM Ltd.) and watered until fully saturated. They were allowed to

drain for two days until approximately at field capacity. Two rhizotrons/replications were planted with TAM111 and two rhizotrons were planted with TAM112. Twelve non-vernalized seeds of a cultivar were planted in a single rhizotron. Once the seedlings were 5 cm tall, they were thinned to six seedlings per rhizotron. The four rhizotrons were arranged in a greenhouse alternating cultivars. The Plexiglass faces were tilted down at a 45° angle so that roots would press against the pane as they grow. The Plexiglass was covered with black fabric to block out sunlight except when measurements were being taken. Every 3 days, the root length, branching width, and branching depth were measured on three seedlings in each rhizotron with the longest roots.

Results

TAM111 had a significantly faster rate of root growth and significantly deeper roots than TAM112 as hypothesized (Figure D-1). No other significant differences in root morphology were found. Rhizotrons provide a convenient way to visualize root growth without destructive sampling. However, it is an artificial environment and does not mimic soil properties that exist under field conditions. Nonetheless, these findings warrant further investigation aimed at determining whether differences in rooting depth between TAM111 and TAM112 exist under field conditions and whether a deeper root system contributes to drought tolerance of TAM111.

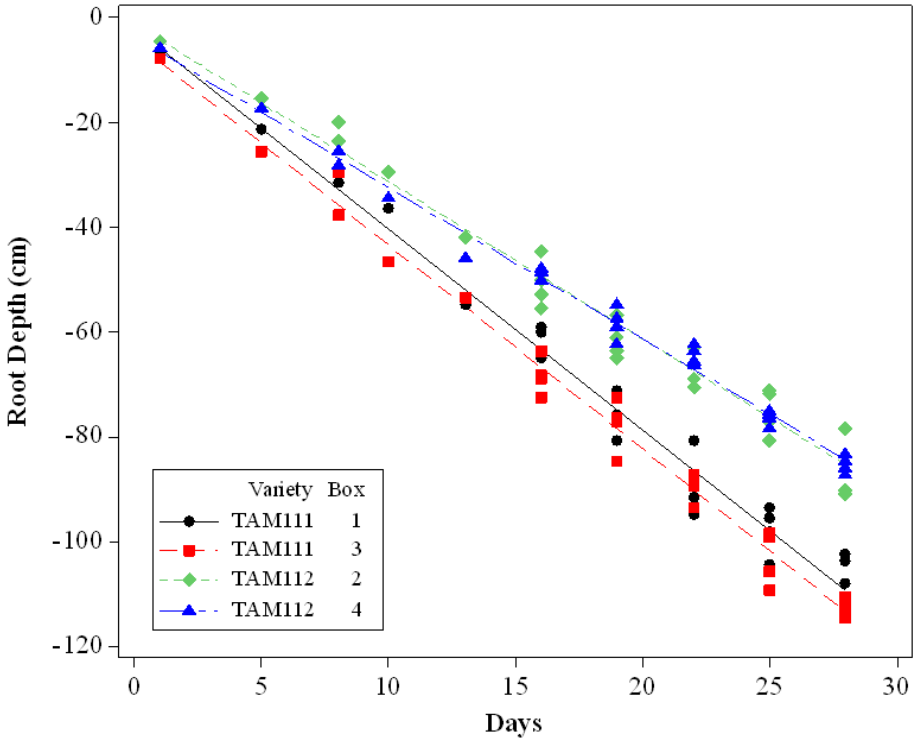

Figure D-1. Rooting depth of non-vernalized TAM111 and TAM112 seedlings over time grown in rhizotrons under greenhouse conditions. Only three plants with the longest roots out of six of each cultivar were measured.

Figure D-2. Two rhizotrons each with 6 plants of TAM111 and two rhizotrons each with 6 plants of TAM112 non-vernalized winter wheat seedlings growing in rhizotrons in a greenhouse.

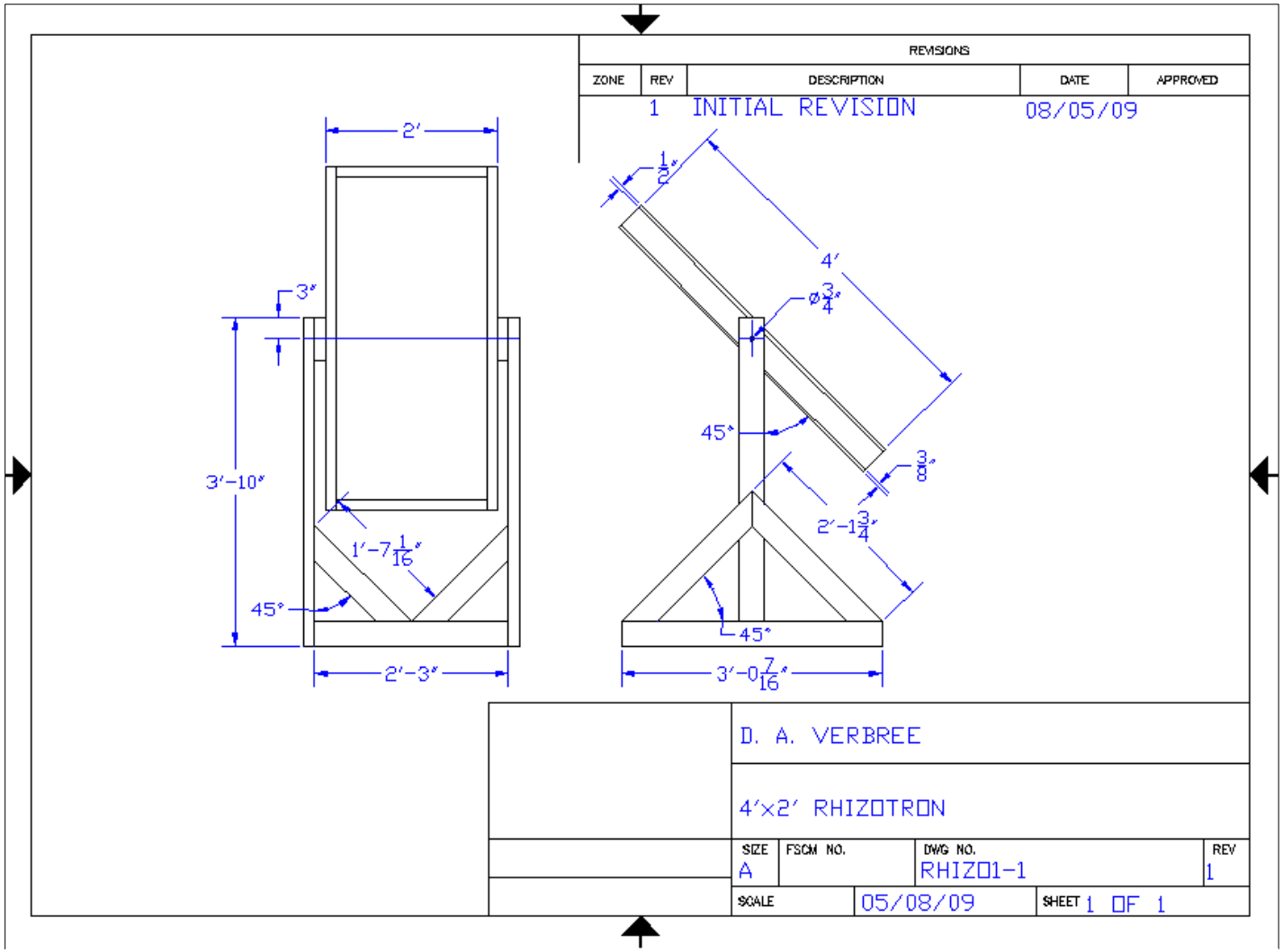

Figure D-3. Rhizotron design.

APPENDIX E

METHOD OF CONTINUOUS PHENOTYPING OF CANOPY TEMPERATURE IN COWPEA USING THERMAL IMAGING

Canopy temperature has been used as an indicator of transpiration and overall plant water status in several species. However, it is unknown whether significant differences can be found among cowpea cultivars. It is also unknown at what time of day and at what level of water stress is most appropriate to take canopy temperature measurements in cowpea. Several drought tolerant and drought susceptible cultivars identified in Section 2 were screened under growth room conditions using the box method described in Section 2. A thermal camera with a wide-angle lens was placed on a tripod and configured to record images every 30 minutes 24 hours day^{-1} for the duration of water stress (Figure E-1). The data was analyzed using custom software described in Section 4 (Figure E-2).

There was only a 7-day window (from 38-45 days of stress), during which significant differences between cultivars could be found. During that window, one drought tolerant cultivar, TX2028-1-3-1, and one drought susceptible cultivar, IT97k-556-4, were significantly hotter than the other drought susceptible cultivars during the daytime (Table E-1). The same drought tolerant cultivar and a different drought susceptible cultivar, CB46, were significantly hotter than the other drought susceptible cultivars during the nighttime. The canopy temperature range of all cultivars was only 0.5° C and therefore, any differences in canopy temperature may have little practical

significance in conferring drought tolerance. Nonetheless, continuous phenotyping of canopy temperature may greatly increase precision and detect significant differences between cultivars that differ by only a fraction of degree.

Figure E-1. Thermal camera on a tripod in a grown room configured to record thermal images of cowpea seedlings every 30 minutes 24 hours day^{-1} under drought box screening conditions.

Table E-1. Average day and night time canopy temperatures of cowpea cultivars from 38 to 45 days of water stress. During this period of time, significant differences between cultivars were found using the general linear model with repeated measures and a Tukey-Kramer means analysis.

	Avg. temperature				
Cultivar	Day		Night		Drought tolerance
	°C				
IT97K-556-4	31.02	b	21.49	a	moderately susceptible
TVu-7778	30.62	a	21.44	a	very susceptible
IT98D-1399	30.48	a	21.39	a	somewhat tolerant
TX2028-1-3-1	31.01	b	21.68	b	very tolerant
CB46	30.53	a	21.76	b	moderately susceptible

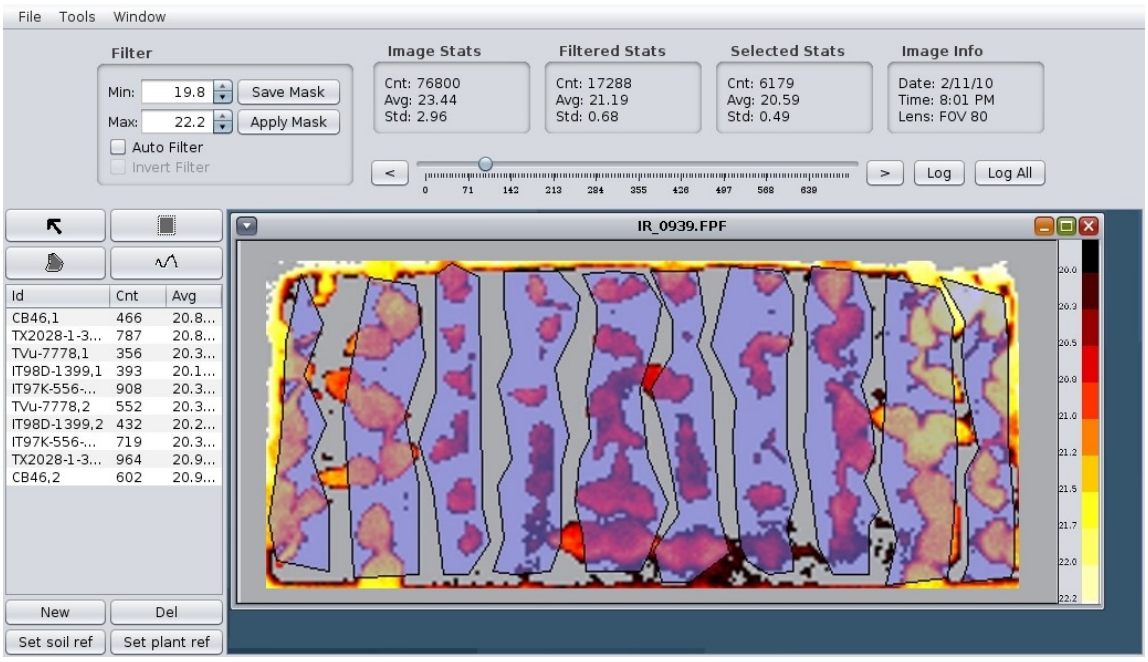

Figure E-2. Screenshot of custom software to automatically filter out soil and analyze over 700 thermal images of 2 replications of 6 plants of 5 cowpea cultivars in a growth room under terminal water stress conditions.

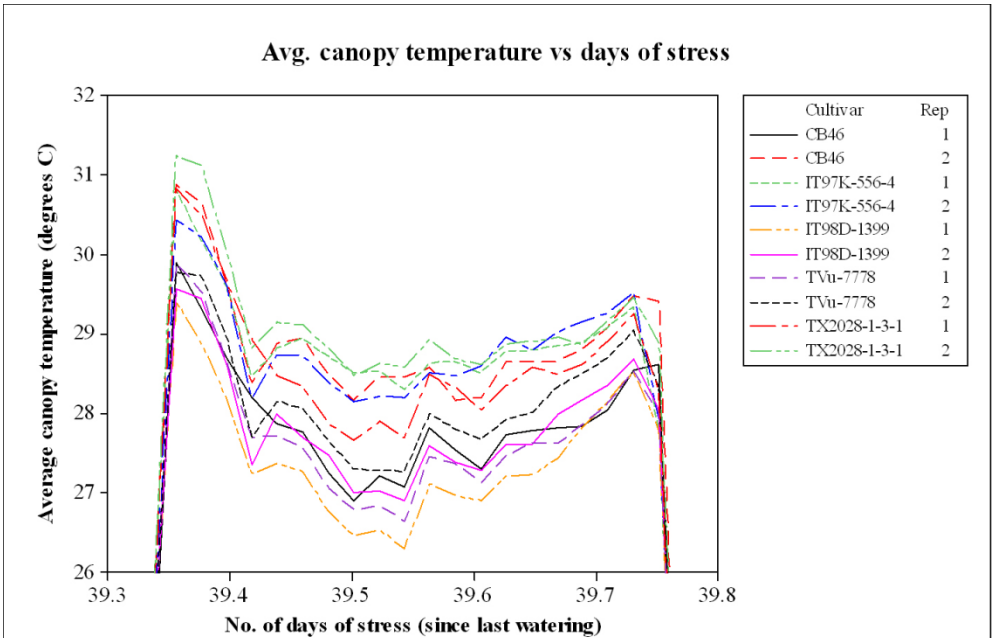

Figure E-3. Example daytime canopy temperature log of two replications of six plants of five cowpea cultivars grown in a shallow box in a growth room on day 39 of water stress.

APPENDIX F

FIELD TRIAL OF COWPEA CULTIVARS AND BREEDING LINES IN COLLEGE STATION, TEXAS

Cowpea field trials were conducted in 2009 at the Texas AgriLife Agronomy Farm in College Station, TX. The field consisted of silty-clay loam soil. Two trials were conducted – an early-maturity yield trial (EM) and a release-candidate yield trial (RC). The EM trial consisted of 20 cultivars arranged in a randomized complete block design (RCBD) with 4 blocks/replications. The RC trial consisted of 24 release-candidates and 7 released cultivars for checks arranged in a RCBD with 5 blocks/replications. In the previous fall, the field was bedded up into rows, 0.76 m apart. In the spring, the field was sprayed with glyphosate, a trifluralin pre-emergent herbicide, and a liquid pop-up fertilizer was applied. Each plot consisted of a single 7.6-m row. The ER trial was planted at 14,100 seeds ha^{-1} (15 cm between seeds) whereas the RC trial was planted 7,050 seeds ha^{-1} (30 cm between seeds). The least significant difference was calculated for each trial.

The pre-emergent herbicide controlled weeds for approximately 3 weeks. By 4 weeks after planting, pigweed (*Amaranthus palmeri*) became a problem. The field was cultivated using a rotary harrow followed by two passes of manual hoeing. Both trials were harvested by hand in two-passes of the first flush of pods for each cultivar.

Table F-1. Results from an early-maturity cowpea yield trial conducted at AgriLife Research Agronomy Farm in College Station, TX.

Cultivar	Seed yield* (kg/ha)
Golden Eye Cream	409
KVx61-1	333
Mouride	294
Coronet	231
Melakh	229
IT82D-889	211
IT98K-589-2	204
Texas Pinkeye	192
CB46	185
TX2044-6-5-1	177
White Acre	174
IT97K-499-35	173
IT97K-1042-3	147
TX2028-1-3-1	144
TX123 Blackeye	143
IT82D-889-1	119
IT98K-1111-1	106
IT98K-205-8	104
Greenpack DG	48
Mean	**191**
LSD (5%)	**97.1**

* 25-ft single-row plots on 30-inch rows, 4 replications in RCBD, planted 2 seed per foot (14,100 seeds/ha)

Table F-2. Results from a release-candidate cowpea yield trial conducted at AgriLife Research Agronomy Farm in College Station, TX.

Cultivar	Seed yield* (kg/ha)
Golden Eye Cream	167
Speckled Purple Hull	157
TX08-49-3	146
TX08-74-1	139
TX08-4-1	121
TX08-30-8	120
Texas Pinkeye	118
TX08-30-2	116
TX08-4-2	115
TX08-13-2	114
TX164 Blackeye	112
TX08-13-1	111
TX08-30-1	105
TX08-49-1	101
TX08-13-3	99
TX08-30-5	94
TX08-30-7	93
TX08-4-3	91
TX08-30-9	88
CB46	83
TX08-30-6	80
TX08-30-4	79
TX123 Blackeye	73
TX08-13-4	73
TX2028-1-3-1	67
TX08-4-5	65
TX08-4-4	62
TX08-49-2	54
TX08-30-3	53
TX08-13-5	49
TX08-4-6	33
Mean	**96**
LSD (5%)	**44.3**

* 25-ft single-row plots on 30-inch rows, 5 replications in RCBD, planted 1 seed per foot (7,050 seeds/ha)

VITA

Name: David Adrian Verbree

Address: 340 Olsen Blvd. 2474 TAMU College Station, Texas 77845-2474

Email Address: david.verbree@tamu.edu

Education:

Ph.D., Plant Breeding, Texas A&M University, exp. May 2012
- Diversity Fellow and Graduate Assistant – Research
- Dissertation title: "Physiology and Genetics of Drought Tolerance in Cowpea and Winter Wheat"

M.S., Agronomy, The Pennsylvania State University, 2008
- Research Assistant
- Thesis title: "Sediment and Nutrient Losses in Reduced Tillage Systems on Dairy Farms"

B.S., Computer Science, Calvin College, 1999

Experience:

2004-present – Verbree International, Burkina Faso ,W. Africa
- Executive Director and Founder of NGO conducting agricultural development projects in dryland W. Africa

2003-2005 – DornerWorks Ltd., Grand Rapids, MI
- Engineer Contractor – contracted to Smiths-Aerospace (now GE Aviation)
- Designed files systems and device drivers for flight management systems

2002-2003 – Shelter for Life International, Afghanistan
- Administered grants, offices, and over 40 national engineers and support staff in Herat, Ghor, and Badghis provinces
- Conducted surveys and assessments in remote villages

1998-2002 – Smiths Industries –, Grand Rapids, MI
- Designed flight simulators and device drivers for embedded systems

Selected Publications: Verbree, D.A., S. Duiker, P. Kleinman. 2010. Runoff losses of sediment and phosphorus from no-till and cultivated soils receiving dairy manure. *Journal of Environmental Quality*. 39: 1762-1770.

Selected Presentations: ASA-CSSA-SSSA in 2008 (poster), 2010 (invited), and 2011 (oral).